Polymers interacting with spherical and rodlike particles

E. Eisenriegler

Andreas Hanke
The University of Texas Rio Grande Valley

S. Dietrich

Recommended Citation

Eisenriegler, E.; Hanke, Andreas; and Dietrich, S., "Polymers interacting with spherical and rodlike particles" (1996). *Physics and Astronomy Faculty Publications and Presentations*. 386.
https://scholarworks.utrgv.edu/pa_fac/386

Polymers interacting with spherical and rodlike particles

E. Eisenriegler

Institut für Festkörperforschung, Forschungszentrum Jülich, D-52425 Jülich, Federal Republic of Germany

A. Hanke and S. Dietrich

Fachbereich Physik, Bergische Universität Wuppertal, D-42097 Wuppertal, Federal Republic of Germany

The interaction of a long flexible polymer chain with mesoscopic particles of spherical or elongated cylindrical shape is investigated by field-theoretic methods using the polymer-magnet analogy. In the case that these particles are immersed in a dilute polymer solution and exhibit purely repulsive surfaces we study density profiles for monomers and chain ends near such a particle, the change of configurational entropy by immersing a particle into the solution, and the depletion interaction between a particle and a distant planar wall. Both ideal chains and chains with an excluded-volume interaction are considered. We also analyze particle surfaces with a short-ranged attraction and the adsorption-desorption transition for an ideal polymer chain. Properties such as the number of surface contacts are evaluated both in the adsorbed limit, in which the thickness of the adsorbed layer is much smaller than the unperturbed polymer size so that ground-state dominance applies, and at the adsorption threshold. [S1063-651X(96)02308-2]

I. INTRODUCTION

Due to the importance for both basic research and applied science the behavior of polymers near surfaces or interfaces has been studied extensively both theoretically [1–6] and experimentally [3,6]. Besides planar surfaces, in this context increasing attention has been devoted to *curved* surfaces such as those of spherical [7] or rodlike [8] colloidal particles. This comprises ''single chain'' problems both for repulsive [9] and attractive [10,11] surfaces as well as situations involving many chains [12,13] and more than one particle [14,15].

Apart from lattice-based methods [5,6], the field-theoretic continuum approach to polymer statistics is well established [4,16]. In this contribution we show that this field-theoretic approach, which has been already applied to study the properties of polymers near planar substrates, can be extended successfully to geometries with curved boundaries such as those of spheres and cylinders. Although the major part of our study will concentrate on *ideal* chains, important results are also derived for chains with an excluded-volume interaction (EVI). Experimentally, almost ideal polymer chains are realized by the so-called ''Θ polymers'' [1,16] for which the actual self-avoidance is nearly compensated by an attractive monomer interaction. In addition in many cases the ideal chain model serves as a starting point for a perturbative treatment of EVI [16].

We shall show that within the continuum approach nontrivial phenomena that curved boundaries induce for polymer chains can be derived systematically. In particular we discuss the behavior of a single ideal chain near a spherical or a cylindrical surface endowed with a short-ranged attractive potential. Properties of its adsorbed state such as the chain extension perpendicular to the surface or the fraction of adsorbed monomers in contact with the surface, which have been considered in Refs. [10] and [11], arise as special cases. For purely repulsive surfaces we consider a dilute solution of free chains for chains both with and without EVI. It turns out that important properties that have originally been discovered in the context of field theory can be used also in the present problem of polymer chains near curved boundaries. In particular we discuss the polymer behavior arising both in close proximity to the surface and in the limit in which the particle has a ''small'' radius [17].

We consider a geometry in which the volume $V \subset \mathbb{R}^D$ accessible to the polymers is the outer space

$$V = \{\mathbf{r} = (\mathbf{r}_\perp, \mathbf{r}_\parallel) \in \mathbb{R}^d \times \mathbb{R}^{D-d}; r_\perp \equiv |\mathbf{r}_\perp| > R\} \qquad (1.1)$$

of a *generalized cylinder* K in $[d + (D-d)]$-dimensional space with radius R and is bounded by the *surface* $S = \partial K$ of the generalized cylinder. For the time being we restrict D and d to integer values $1, 2, 3, \ldots$ with $d \leq D$. Special cases of this geometry are the outer space of a D-dimensional sphere with radius R ($d = D$) and the outer space of a D-dimensional cylinder with radius R ($d = D-1$), which is a genuine cylinder for $D = 3$ (see Fig. 1). Note that for $d = 1$ the generalized cylinder K is a plate of width $2R$ and the volume V consists of two disconnected half spaces so that the geometry degenerates to the *semi-infinite geometry*, which has been studied in much detail (see, e.g., Ref. [4] for a review). While only the cases $D = 2$ and $D = 3$ are experimentally relevant, the case $D = 4$ is of theoretical interest because $D = 4$ marks the upper critical dimension for the relevance of EVI in the bulk [1,16].

Within the continuum description [18] the *partition function* [19] $Z_L(\mathbf{r}, \mathbf{r}')$ of an *ideal* chain with a fixed monomer number characterized by L [20] and fixed ends at $\mathbf{r}, \mathbf{r}' \in V$ is symmetric in $\mathbf{r}, \mathbf{r}'$ and satisfies the diffusion-type equation

$$\left(\frac{\partial}{\partial L} - \Delta_D\right) Z_L(\mathbf{r}, \mathbf{r}') = 0 \qquad (1.2a)$$
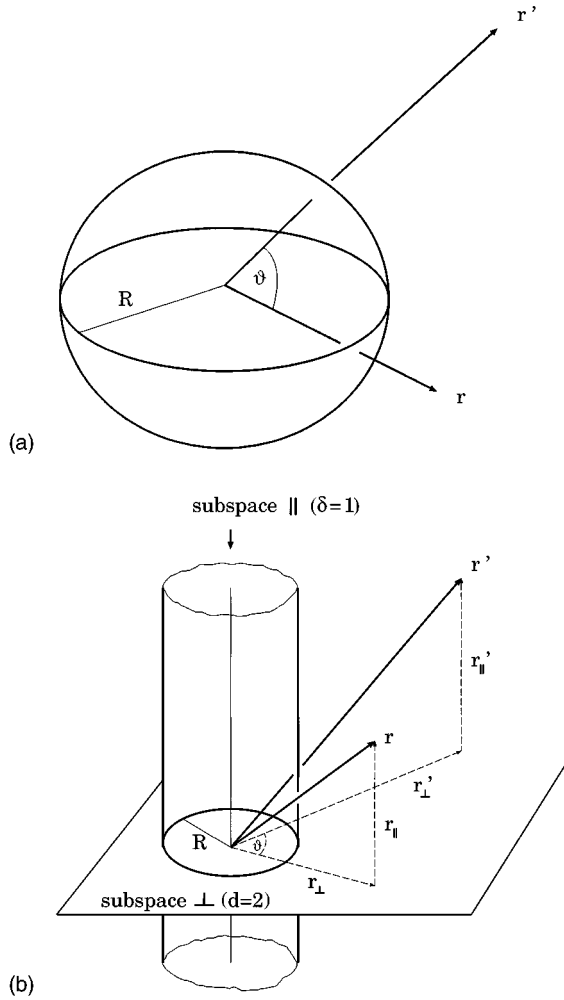
with the ''initial condition''

(a)

(b)

FIG. 1. A sphere (a) and a cylinder (b) as examples of particles with curved boundaries. The two spatial arguments $\mathbf{r}$ and $\mathbf{r}'$ of the partition function Z_L in Eq. (1.2) are also shown.

$$Z_{L=0}(\mathbf{r},\mathbf{r}') = \delta^{(D)}(\mathbf{r}-\mathbf{r}') \qquad (1.2\text{b})$$

and the boundary condition

$$\partial_n Z_L(\mathbf{r},\mathbf{r}')\big|_{\mathbf{r}=\mathbf{r}_S} = c Z_L(\mathbf{r},\mathbf{r}')\big|_{\mathbf{r}=\mathbf{r}_S} \qquad (1.2\text{c})$$

at the surface S. Here Δ_D is the Laplacian operator (which acts on $\mathbf{r} \in V$) and $\delta^{(D)}(\mathbf{r})$ is Dirac's δ distribution in D-dimensional space; ∂_n denotes the derivative normal to the surface towards the interior of V and $\mathbf{r}_S$ is a point on the surface S. The quantity c is an inverse extrapolation length characterizing a short-ranged surface potential [1,2,4] (see Appendix A), which acts only on monomers that are located microscopically close to the surface; the more negative the quantity c, the more *attractive* the surface.

For the present Gaussian (ideal chain) model with the geometry (1.1) the parallel contributions of the partition function Z_L can be split off, i.e.,

$$Z_L(\mathbf{r},\mathbf{r}') \equiv Z_L(\mathbf{r},\mathbf{r}';c,R) = Z_L^{(\perp)}(\mathbf{r}_\perp,\mathbf{r}'_\perp;c,R) Z_{L,b}^{(\delta)}(|\mathbf{r}_\parallel - \mathbf{r}'_\parallel|) \qquad (1.3)$$

where $Z_{L,b}^{(\delta)}$ is the Gaussian partition function in the $\delta \equiv (D-d)$-dimensional unbounded subspace $\mathbb{R}^{D-d}$ of the parallel components of V [19].

It follows from Eq. (1.2) that the Laplace transform

$$G(\mathbf{r},\mathbf{r}';t,c,R) = \int_0^\infty dL e^{-Lt} Z_L(\mathbf{r},\mathbf{r}';c,R) \qquad (1.4)$$

is the two-point correlation function (or *propagator*) $\langle \Phi(\mathbf{r})\Phi(\mathbf{r}') \rangle_{\mathcal{H}_K}$ of a Gaussian field theory with a statistical weight $\exp(-\mathcal{H}_K\{\Phi\})$, where $\mathcal{H}_K\{\Phi\}$ is a Ginzburg-Landau type Hamiltonian [4]

$$\mathcal{H}_K\{\Phi\} = \int_V d^D r \left\{ \frac{1}{2}(\nabla\Phi)^2 + \frac{1}{2}t\Phi^2 \right\} + \int_S dS_\mathbf{r} \frac{1}{2}c\Phi^2 \qquad (1.5)$$

for a scalar order parameter $\Phi(\mathbf{r}) \in \mathbb{R}$. In this ''magnetic'' analogy, where $t \propto (T-T_c^b)/T_c^b$ measures the deviation of the temperature T from the bulk critical temperature T_c^b the quantity $-c$ is related to the surface-coupling enhancement relative to the bulk couplings [21,22]. As above, the position vector $\mathbf{r}$ covers the volume V and its boundary S.

For an ideal chain the mean fraction $d^D y\, m(\mathbf{y})$ of monomers that are located inside the volume element $d^D y$ around $\mathbf{y}$ under the constraint that the two chain ends are fixed at $\mathbf{r}$ and $\mathbf{r}'$, respectively, is determined by [1,4]

$$m(\mathbf{y};\mathbf{r},\mathbf{r}';L,c,R) = \frac{1}{L}\int_0^L dL' Z_{L-L'}(\mathbf{r},\mathbf{y};c,R)$$

$$\times Z_{L'}(\mathbf{y},\mathbf{r}';c,R)/Z_L(\mathbf{r},\mathbf{r}';c,R); \qquad (1.6)$$

in particular one has $\int_V d^D y\, m(\mathbf{y}) = 1$. In the context of the adsorption-desorption transition a quantity of particular interest is the mean fraction $dy_\perp m_\ell$ of monomers in a (curved) layer ℓ of width $dy_\perp$, which is concentric and in ''close proximity'' to the surface. If the distance $y_\perp - R$ of the layer from the surface is much smaller than $|c|^{-1}$, R, and $L^{1/2}$ [23] the continuum model for an ideal chain leads to a $y_\perp$-independent proximal behavior

$$m_\ell(\mathbf{r},\mathbf{r}';L,c,R) = \int_S dS_\mathbf{y}\, m(\mathbf{y};\mathbf{r},\mathbf{r}';L,c,R)$$

$$= \frac{1}{L}\left[-\frac{\partial}{\partial c} Z_L(\mathbf{r},\mathbf{r}';c,R) \right] \bigg/ Z_L(\mathbf{r},\mathbf{r}';c,R). \qquad (1.7)$$

It follows from Eq. (1.7) that c acts like a chemical potential for monomers near the surface.

The remainder of this paper is arranged as follows. We apply the result for the Gaussian propagator G derived in Appendix B [24] in order to obtain the partition function Z_L via an inverse Laplace transform according to Eq. (1.4). In Sec. II we consider a single ideal chain with one end fixed and one end free and derive the phase diagram for polymer adsorption. We discuss the behavior of the monomer fraction layer density $\hat{m}_\ell$, which is the counterpart of m_ℓ introduced above for the case in which the chain is fixed with one end only. Both an infinitely long chain in the adsorbed region and

a chain at the adsorption threshold are considered. For the former case we also discuss the behavior of the thickness of the adsorbed layer.

In Sec. III we consider a dilute solution of freely moving chains near a purely repulsive surface for both ideal chains and chains with EVI. We discuss the corresponding end density and monomer density profiles and derive the configurational free energy for the immersion of a spherical or cylindrical particle. In Sec. IV we present analytic expressions for these quantities if the radius R of the particle is ''small'' and address the problem of the interaction of a particle with a planar wall. In Sec. V we present our conclusions.

Appendices A and B are devoted to a discussion of the surface parameter c and the Gaussian propagator G, respectively, in the geometry (1.1). In Appendix C we consider the configurational free energy of polymers near weakly curved repulsive surfaces of general shape.

II. SINGLE CHAIN WITH ONE END FIXED

In this section we consider a single ideal polymer chain with one end fixed while the other end is moving freely.

A. Adsorption-desorption phase diagram

The partition function of a chain with one end fixed at $\mathbf{r} = (\mathbf{r}_\perp, \mathbf{r}_\parallel) \in V$ while the other end is free is given by

$$\hat{Z}_L(r_\perp; c, R) = \int_V d^D r' Z_L(\mathbf{r}, \mathbf{r}'; c, R) = \mathcal{L}_{t \to L}\{\chi(r_\perp; t, c, R)\}.$$

(2.1)

Here $\mathcal{L}_{t \to L}$ denotes an inverse Laplace transform and the *local susceptibility* χ of the magnetic analogue is given by the integrated propagator

$$\chi(r_\perp; t, c, R) = \int_V d^D r' G(\mathbf{r}, \mathbf{r}'; t, c, R)$$

$$= \int_R^\infty dr'_\perp r'^{d-1}_\perp \widetilde{G}_{\ell=0}(r_\perp, r'_\perp; \mu = t, c, R),$$

(2.2)

where $\widetilde{G}_{\ell=0}$ can be read off from Eqs. (B3c) and (B3d) in Appendix B. The second line follows from rotational invariance around and translational invariance along the generalized cylinder. As indicated above, the local susceptibility χ and thus the partition function $\hat{Z}_L$ depend only on the *radial* component $r_\perp = |\mathbf{r}_\perp|$ of the point $\mathbf{r} = (\mathbf{r}_\perp, \mathbf{r}_\parallel)$. It follows from Eq. (1.3) and from the relation $\int_\mathbb{R} d^\delta r_\parallel Z_{L,b}^{(\delta)} = 1$ [19] that the form of this function does *not* depend on $\delta = D - d$ but will depend only on d. This is consistent with our result for $\widetilde{G}_{\ell=0}$ derived in Appendix B.

We introduce dimensionless quantities expressed in terms of the radius R of the generalized cylinder:

$$\rho \equiv r_\perp/R, \quad \tau \equiv tR^2, \quad \zeta \equiv cR, \quad \lambda \equiv L/R^2. \quad (2.3)$$

Note that $\hat{Z}_L$ is already dimensionless and that the Gaussian propagator G has the same units as R^{2-D}. We thus define the dimensionless local susceptibility

$$\mathcal{X}(\rho; \tau, \zeta) = \chi(r_\perp; t, c, R)/R^2$$

$$= \frac{1}{\tau}\left[1 - \frac{\zeta \rho^{-\alpha} K_\alpha(\rho\sqrt{\tau})}{\sqrt{\tau} K_{\alpha+1}(\sqrt{\tau}) + \zeta K_\alpha(\sqrt{\tau})}\right], \quad (2.4a)$$

where Eqs. (2.2), (B3c), and (B3d) have been used. Here K_α and $K_{\alpha+1}$ are modified Bessel functions [25,26] and

$$\alpha = (d-2)/2. \quad (2.4b)$$

In the limit $\rho \to \infty$ the local susceptibility χ approaches the bulk susceptibility $\chi_b = 1/t$ of the Ginzburg-Landau model. In terms of the dimensionless variables the partition function $\hat{Z}_L$ in Eq. (2.1) reads

$$\hat{Z}_L(r_\perp; c, R) = \hat{\mathcal{Z}}_\lambda(\rho; \zeta) = \mathcal{L}_{\tau \to \lambda}\{\mathcal{X}(\rho; \tau, \zeta)\}. \quad (2.5)$$

We also consider the monomer fraction layer density $\hat{m}_\diagup$ near the surface for the present case in which the chain is fixed with one end only. This quantity is given by the last expression in Eq. (1.7) with Z_L replaced by $\hat{Z}_L$, i.e., by

$$\hat{m}_\diagup(r_\perp; L, c, R) = -\frac{1}{R\lambda}\frac{\partial}{\partial\zeta}\ln\hat{\mathcal{Z}}_\lambda(\rho; \zeta). \quad (2.6)$$

Note that the last expression in Eq. (2.4a) is well defined even if $\alpha = (d-2)/2$ is varied *continuously* over the range $\alpha \geq -1/2$, i.e., $d \geq 1$, which we have assumed in the foregoing discussion. This allows us to study the dependence of the partition function and related quantities on the spatial dimension d of the radial subspace.

The expression for the local susceptibility $\mathcal{X}(\rho; \tau, \zeta)$ as given in Eq. (2.4a) is valid only for $\tau > \tau_0(\zeta)$ with

$$\tau_0(\zeta) = \begin{cases} 0, & \zeta \geq \zeta^* \\ p_\alpha(\zeta), & \zeta < \zeta^*. \end{cases} \quad (2.7)$$

The corresponding phase diagram of the Gaussian field theory is shown in Fig. 2(a). The function $p_\alpha(\zeta)$ is positive and decreasing (with increasing ζ), and follows implicitly from the zero of the denominator of the second term in brackets in Eq. (2.4a) [27], i.e.,

$$\sqrt{p_\alpha(\zeta)} K_{\alpha+1}(\sqrt{p_\alpha(\zeta)}) + \zeta K_\alpha(\sqrt{p_\alpha(\zeta)}) = 0 \quad (2.8)$$

while $\zeta^* = \zeta^*(d)$ follows from $\lim_{\zeta \nearrow \zeta^*} p_\alpha(\zeta) = 0$. We find

$$\zeta^*(d) = \begin{cases} 0, & d \leq 2 \\ -(d-2), & d > 2, \end{cases} \quad (2.9a)$$

and the form

$$|\Delta\zeta| = \frac{\sqrt{p_\alpha}}{K_\alpha(\sqrt{p_\alpha})} \times \begin{cases} K_{\alpha+1}(\sqrt{p_\alpha}), & d \leq 2 \\ K_{\alpha-1}(\sqrt{p_\alpha}), & d > 2, \end{cases} \quad (2.9b)$$

from which p_α can be determined as a function of the deviation $\Delta\zeta = \zeta - \zeta^* < 0$. For a cylinder ($d = 2$) one has $c^* = 0$ while for a sphere ($d = 3$) one has $c^* = -1/R$ [28]. For the planar case $d = 1$ and for $d = 3$ Eq. (2.9b) is solved by
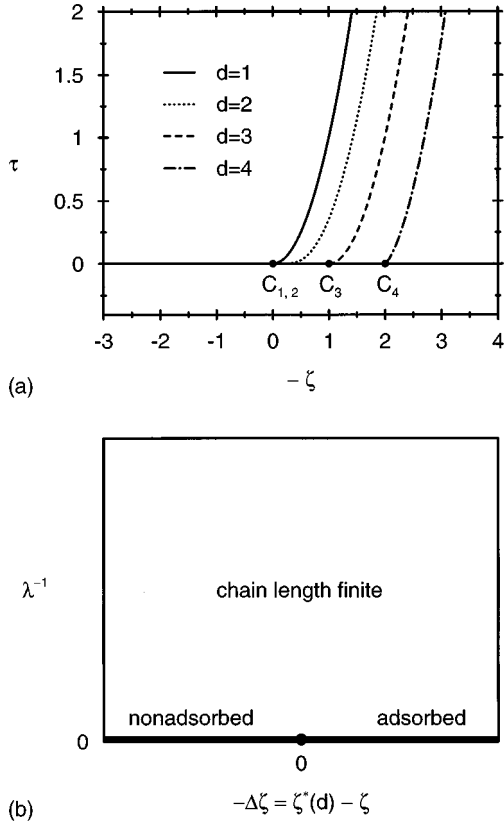
FIG. 2. (a) Phase diagram of the Gaussian field theory [Eqs. (1.5) and (2.3)] for several dimensions d of the radial subspace. The only stable region is the left and upper part, which is bounded by the lines $\tau_0(\zeta)$ and which corresponds to a bulk disordered and surface disordered magnetic phase [21,22]. The curved lines are plots of the function $p_\alpha(\zeta)$ in Eq. (2.7); the points C_d are multicritical points. (b) Corresponding adsorption-desorption phase diagram of an ideal polymer chain in terms of $\lambda^{-1}=R^2/L$ and $\zeta=cR$. In the limit of an infinite chain length ($\lambda^{-1}=0$) a finite fraction of the chain is adsorbed on the surface for $\zeta<\zeta^*$ whereas this fraction vanishes for $\zeta>\zeta^*$. The corresponding transition at $\zeta=\zeta^*$ is the so-called adsorption-desorption transition. The basic mechanism that relates these behaviors of the field theory and the polymer system is discussed near Eqs. (2.12) and (2.13).

$p_\alpha(\zeta)=(\Delta\zeta)^2$ [26]. For $d=2$ and $d=4$ Eq. (2.9b) can be solved analytically for p_α only in the limit $\zeta\nearrow\zeta^*$ for which we find

$$p_{\alpha=0}(\zeta\nearrow\zeta^*)\simeq 4e^{-2C}e^{-2/|\Delta\zeta|}, \quad d=2, \quad (2.10)$$

where $C=0.5772\cdots$ denotes Euler's constant, and

$$p_{\alpha=1}(\zeta\nearrow\zeta^*)\simeq -\frac{2|\Delta\zeta|}{\ln(|\Delta\zeta|)}, \quad d=4, \quad (2.11)$$

with $\zeta^*(d=2)=0$ and $\zeta^*(d=4)=-2$. For $d>4$ we infer the behavior $p_\alpha(\zeta\nearrow\zeta^*)\simeq(d-4)|\Delta\zeta|$.

If ζ is more negative than ζ^* (i.e., if the attractive surface potential is sufficiently large) the local susceptibility $\mathcal{X}(\rho;\tau,\zeta)$ diverges for $\tau\searrow p_\alpha(\zeta)$. In this case the direct transform

$$\mathcal{X}(\rho;\tau,\zeta)=\int_0^\infty d\lambda\, e^{-\lambda\tau}\hat{\mathcal{Z}}_\lambda(\rho;\zeta) \quad (2.12)$$

corresponding to Eq. (2.5) yields a behavior $\hat{\mathcal{Z}}_\lambda \sim\exp[\lambda p_\alpha(\zeta)]$ for $\lambda\to\infty$, which implies $\hat{m}_\angle R\sim\lambda^0$ according to Eq. (2.6) and thus a *finite* asymptotic fraction density

$$P(c,R)\equiv\lim_{L\to\infty}\hat{m}_\angle(r_\perp;L,c,R) \quad (2.13)$$

of adsorbed monomers for $\zeta<\zeta^*$. Since $P(c,R)$ has the dimension of an inverse length we define the corresponding dimensionless quantity as $\mathcal{P}(\zeta)\equiv RP(c,R)$.

For $\zeta>\zeta^*$, however, $\hat{\mathcal{Z}}_\lambda$ does not increase exponentially as a function of λ so that one has $\hat{m}_\angle R\sim\lambda^{-1}$ for $\lambda\to\infty$ and $P(c,R)$ vanishes in this limit. This will be verified in detail in the next subsection [c.f. the discussion corresponding to Eq. (2.16)]. Thus the "magnetic" phase diagram of Fig. 2(a) translates into a phase diagram for polymer adsorption in the $(\lambda^{-1}, -\zeta)$ plane [Fig. 2(b)] with a nonvanishing (vanishing) asymptotic fraction density $\mathcal{P}(\zeta)$ of monomers adsorbed on the surface for $\zeta<\zeta^*$ ($\zeta>\zeta^*$).

Here we note that for an *attractive* surface of a *sphere* (which is completely finite) and chains with excluded-volume interaction the above results will be strongly modified (see the discussion in Ref. [10] and in Sec. V below). In particular, for a chain with EVI, we expect a nonzero asymptotic adsorbed fraction density $\mathcal{P}(\zeta)$ only for $d\leq D-1$ which includes a cylindrical surface for which $D=3$ and $d=2$.

Finally we note that for $d=1$ and for $d=3$ the expression for the local susceptibility in Eq. (2.4a) reduces to [26]

$$\mathcal{X}(\rho;\tau,\zeta)=\frac{1}{\tau}\left[1-\omega\frac{\zeta e^{-\sqrt{\tau}(\rho-1)}}{\sqrt{\tau}+\Delta\zeta}\right], \quad d=1,3, \quad (2.14)$$

where $\omega=1$ for $d=1$ and $\omega=\rho^{-1}$ for $d=3$, respectively, and $\Delta\zeta$ has been defined below Eq. (2.9b). Accordingly the inverse Laplace transform in Eq. (2.5) can be performed explicitly [29] with the result [30]

$$\hat{\mathcal{Z}}_\lambda(\rho;\zeta)=1+\omega\frac{\zeta}{\Delta\zeta}\{\exp[(\Delta\zeta)^2\lambda+2\Delta\zeta\lambda^{1/2}\gamma]$$
$$\times\operatorname{erfc}(\Delta\zeta\lambda^{1/2}+\gamma)-\operatorname{erfc}\gamma\}, \quad d=1,3,$$
$$(2.15a)$$

where

$$\gamma\equiv(r_\perp-R)/(2L^{1/2})=(\rho-1)/(2\lambda^{1/2}); \quad (2.15b)$$

erfc denotes the complementary error function [25].

B. Fraction density and layer thickness ($c<c^*$)

By using transfer matrix techniques Boettcher and Moshe [11] studied a one-dimensional lattice model in order to derive the finite adsorbed fraction in the limit $L\to\infty$ of an ideal polymer chain positioned near a cylindrical boundary. In the following we derive the corresponding quantity $P(c,R)$ in the continuum description. We first note that for $\zeta\neq\zeta^*$ the inverse Laplace transform [4,16] in Eq. (2.5) can be performed for general d up to a one-dimensional integral:

$$\hat{\mathcal{Z}}_\lambda(\rho;\zeta) = \frac{2\alpha+\zeta(1-\rho^{-2\alpha})}{2\alpha+\zeta}\Theta(\alpha) + \rho^{-\alpha}[K_\alpha(\rho\sqrt{p_\alpha(\zeta)})/K_\alpha(\sqrt{p_\alpha(\zeta)})]\frac{2|\zeta|e^{\lambda p_\alpha(\zeta)}}{\zeta(\zeta+2\alpha)-p_\alpha(\zeta)}\Theta(\zeta^*-\zeta)$$

$$+ \frac{2\zeta}{\pi}\int_0^\infty dx\,\frac{e^{-\lambda x^2}}{x}\,\mathrm{Im}\left[\frac{\rho^{-\alpha}H_\alpha^{(1)}(\rho x)}{xH_{\alpha+1}^{(1)}(x)+\zeta H_\alpha^{(1)}(x)}\right], \quad \zeta\neq\zeta^*, \tag{2.16}$$

where $H_\alpha^{(1)}$ denotes a Hankel function [25] and $\Theta(x)$ is the Heaviside step function. The second term on the right-hand side (rhs) increases exponentially as a function of λ and arises from a pole at $\tau=p_\alpha(\zeta)$ appearing in $\mathcal{X}(\rho;\tau,\zeta)$ for $\zeta<\zeta^*$ [see the discussion corresponding to Eq. (2.12)]. In the long chain limit $\lambda\to\infty$ and for $\zeta<\zeta^*$ this term is the dominating one and Eqs. (2.6), (2.13), and (2.16) lead to [31]

$$RP(c,R)=\mathcal{P}(\zeta)=-\frac{d}{d\zeta}p_\alpha(\zeta)=\frac{2p_\alpha(\zeta)}{\zeta(\zeta+2\alpha)-p_\alpha(\zeta)}. \tag{2.17}$$

Equation (2.17) is to be compared with Eq. (9) in Ref. [11(a)]. The expression (2.17) for $P(c,R)$ *does* exhibit a manifest *scaling* form for which dimensional analysis tells us that $RP(c,R)$ depends only on the *product* of the two variables c and R.

In order to facilitate the comparison of our results with those of Ref. [11] we use the original (unscaled) variables c and R and the adsorption fraction density $P(c,R)$. For $d=1$ and $d=3$ we obtain [26] for arbitrary $\Delta c=c-c^*<0$

$$P(c,R)=2|\Delta c|, \quad d=1,3, \tag{2.18}$$

where $c^*(d=1)=0$ and $c^*(d=3)=-1/R$. For $d=2$ and $d=4$ Eqs. (2.10) and (2.11) lead to [32]

$$P(c\nearrow c^*,R)\simeq\frac{8}{R^3|\Delta c|^2}e^{-2C}e^{-2/(|\Delta c|R)}, \quad d=2, \tag{2.19}$$

and

$$P(c\nearrow c^*,R)\simeq-\frac{2}{R\ln(|\Delta c|R)}, \quad d=4, \tag{2.20}$$

where $c^*(d=2)=0$ and $c^*(d=4)=-2/R$.

In Refs. [11(a),(b)] results for $d=2$ have been reported in which the dependences on the radius R in the prefactors of the exponential terms are *different* (by a factor R^2 for large R on a microscopic scale [18,23]) from those in Eqs. (2.10) and (2.19). This difference can be traced back to a slight error in Refs. [11(a),(b)], which we examine in Ref. [33]. Within the continuum approach the power laws for R follow already from dimensional analysis. For $1\leq d<4$, $d\neq2$, we find in agreement with Ref. [11] that the fraction density scales as $RP(c\nearrow c^*,R)\sim(|\Delta c|R)^\kappa$ with an exponent $\kappa=(2-|d-2|)/|d-2|$ while for $d>4$ it approaches a finite value, $RP(c\nearrow c^*,R)\simeq d-4$. Thus in this case the adsorbed fraction density is a discontinuous function of c. (However, this first-order transition is not realized in physical systems with $d\leq3$.) Mathematically the exceptional asymptotic be-

haviors of $P(c\nearrow c^*,R)$ for $d=2$ and 4 are due to the asymptotic behavior of the modified Bessel function $K_0(z\to0)\simeq-\ln z$.

Figure 3(a) shows the behavior of the scaling function $\mathcal{P}(\zeta)$ for arbitrary $\zeta<\zeta^*$ and for several dimensions d of the radial subspace. For $d=2$ and $d=4$ we have solved Eq. (2.9b) numerically. Note that the behavior of $\mathcal{P}(\zeta\nearrow\zeta^*)$ depends strongly on d. In particular for $d=2$ the fraction vanishes exponentially [11,32]. On the other hand one has, for all d, $\mathcal{P}(\zeta\to-\infty)\simeq2|\zeta|$. This is plausible since in this limit the thickness of the adsorption layer is much smaller than the radius R and the surface is effectively planar.

(a)

(b)
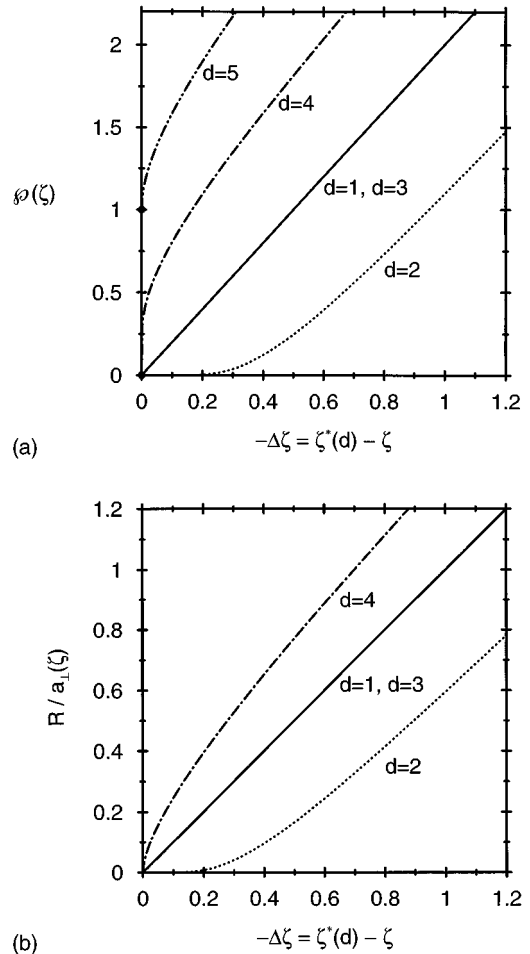
FIG. 3. Crossover scaling functions $\mathcal{P}(\zeta)$ of the adsorbed monomer fraction density (a) and $R/a_\perp(\zeta)$ of the inverse decay length characterizing the thickness of the adsorption layer (b), respectively, for an ideal chain in the adsorbed limit $L\to\infty$, $c<c^*$ and for several dimensions d of the radial subspace. For $d=2$ the fraction density $\mathcal{P}(\zeta\nearrow\zeta^*)$ vanishes exponentially, which corresponds to an exponential divergence of the length $a_\perp$. Note that for $d=5$ the fraction density $\mathcal{P}(\zeta\nearrow\zeta^*)$ approaches a finite value.

A quantitative measure for the thickness of the adsorption layer is provided by the exponential decay length $a_\perp \equiv R/\sqrt{p_\alpha(\zeta)}$ governing the second term on the rhs of Eq. (2.16). The behavior of $R/a_\perp(\zeta) = \sqrt{p_\alpha(\zeta)}$ for several dimensions d of the radial subspace is shown in Fig. 3(b). In particular for $d=2$ the length $a_\perp$ diverges exponentially as $(R/2)e^C e^{1/(|c|R)}$ for $c \nearrow 0$ [34]. For $c \to -\infty$ one has, for all d, $a_\perp \simeq 1/|c|$ as for a planar surface.

C. Number of adsorbed monomers for $c = c^*$

Apart from the behavior of the adsorbed fraction density $\hat{m}_\nearrow$ along the adsorption line ($\zeta < \zeta^*$, $\lambda = \infty$) as considered above it is of interest how this quantity behaves upon approaching the special point ($\zeta = \zeta^*$, $\lambda = \infty$) by increasing λ if ζ is fixed at ζ^*. Here we consider the related dimensionless quantity $\hat{\lambda}_S(\rho; \lambda, \zeta) = \hat{m}_\nearrow L/R$, which is proportional to the number n_S of monomers microscopically close to the surface [23]. For $\zeta = \zeta^*$ the dimensionless local susceptibility in Eq. (2.4a) takes the form

$$\mathcal{X}(\rho; \tau, \zeta^*) = \frac{1}{\tau}\left[1 + \frac{2\alpha\rho^{-\alpha}K_\alpha(\rho\sqrt{\tau})}{\sqrt{\tau}K_{\alpha-1}(\sqrt{\tau})}\Theta(\alpha)\right] \tag{2.21a}$$

while in view of Eq. (2.6)

$$-\frac{\partial}{\partial\zeta}\mathcal{X}(\rho; \tau, \zeta)\Big|_{\zeta=\zeta^*} = \frac{\rho^{-\alpha}}{\tau^{3/2}}K_\alpha(\rho\sqrt{\tau})$$

$$\times \begin{cases} 1/K_{\alpha+1}(\sqrt{\tau}), & d \leq 2 \\ K_{\alpha+1}(\sqrt{\tau})/[K_{\alpha-1}(\sqrt{\tau})]^2, & d > 2. \end{cases} \tag{2.21b}$$

Using Eqs. (2.5) and (2.6) we find the following asymptotic behavior for $\lambda \to \infty$:

$$\hat{\lambda}_S(\rho; \lambda \to \infty, \zeta^*) \simeq \begin{cases} (2/\sqrt{\pi})\lambda^{1/2}, & d=1, \\ (1/2)\ln(4e^{-C}L/r_\perp^2), & d=2, \\ (\sqrt{\pi}/2)\lambda^{1/2}, & d=3, \\ \lambda/\ln\lambda, & d=4. \end{cases} \tag{2.22}$$

We note that for $d=2$ (cylinder) the leading asymptotic behavior for $L \to \infty$ does not depend on the cylinder radius R but does depend on the radial component $r_\perp$ of the point where one end of the chain is fixed. The expressions for $d=1$ and 3 and arbitrary (ρ, λ) follow from Eq. (2.15a). The result for the planar case $d=1$ is also given in Ref. [4].

For $1 \leq d < 4$, $d \neq 2$, we find that $\hat{\lambda}_S(\rho; \lambda, \zeta^*)$ scales as $\lambda^{|\alpha|}$ with $|\alpha| = |d-2|/2$ while for $d > 4$ we infer the behavior $\hat{\lambda}_S \simeq (\alpha-1)\lambda$. This implies that for $d > 4$ and $\lambda \to \infty$ the dimensionless adsorbed fraction density $\hat{m}_\nearrow/R = \hat{\lambda}_S(\rho; \lambda, \zeta^*)/\lambda$ approaches the finite value $(d-4)/2$, which differs from the value $d-4$, which follows upon approaching the special point ($\zeta = \zeta^*$, $\lambda = \infty$) along the adsorption line (see Sec. II B). This means that for $d > 4$ the adsorbed fraction density at the special point ($\zeta = \zeta^*$, $\lambda = \infty$) depends on the *path* in the phase diagram
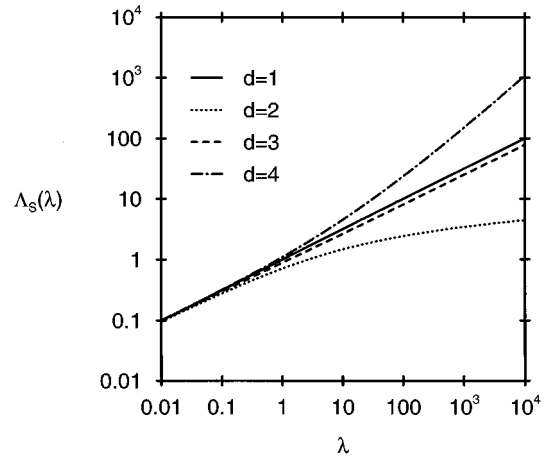

FIG. 4. Crossover scaling function $\Lambda_S(\lambda)$ for the mean number of adsorbed monomers of an ideal chain at $\zeta = \zeta^*$ for several dimensions d of the radial subspace. The curves clearly show the crossover from the planar limit $\lambda \ll 1$ to the long chain limit $\lambda \gg 1$.

along which this point is approached; this is in accordance with the fact that for $d > 4$ the adsorption-desorption transition is first order.

Figure 4 shows the behavior of $\hat{\lambda}_S(\rho; \lambda, \zeta^*)$ for the special case $\rho = r_\perp/R = 1$ and for several dimensions d of the radial subspace in terms of the function

$$\Lambda_S(\lambda) \equiv \frac{1}{2}\sqrt{\pi}\hat{\lambda}_S(\rho=1; \lambda, \zeta^*) \tag{2.23}$$

so that $\Lambda_S(\lambda) = \lambda^{1/2}$ for $d=1$. The curves clearly show the crossover from the planar limit $\lambda = L/R^2 \ll 1$ to the long-chain limit $\lambda \gg 1$ of Eq. (2.22).

Figures 3 and 4 show that $\hat{\lambda}_S(\rho; \lambda \to \infty, \zeta)$ is smallest for $d=2$. The decrease in $\hat{\lambda}_S$ for d increasing between 1 and 2 is plausible since more free space and entropic gain is available for an unbinding chain around a cylinder than near a planar wall. To understand the increase in $\hat{\lambda}_S$ as d increases beyond 2 one has to take into account that in this case $-\zeta^*$, which is related to the attractive surface potential at the threshold, increases with d, too [see Eq. (2.9a)]. For example, the curves for $d=3$ would be located *below* the curves for $d=2$ if $-\zeta$ instead of $-\Delta\zeta$ was used as the abscissa in Fig. 3.

III. DILUTE SOLUTION OF FREE CHAINS NEAR A PURELY REPULSIVE SURFACE

In this section we discuss a dilute solution of freely moving polymer chains near a purely repulsive surface.

A. End density

The density of chain ends at the point $\mathbf{r}$ in a dilute solution of freely moving chains without mutual interaction exhibits a dependence on $\mathbf{r}$ that is proportional to that of the Boltzmann-weighted number of configurations of a single chain with one end fixed at $\mathbf{r}$. For ideal chains moving in the volume V introduced in Eq. (1.1) the density of chain ends is thus proportional to the partition function $\hat{Z}_L$ in Eq. (2.1). In
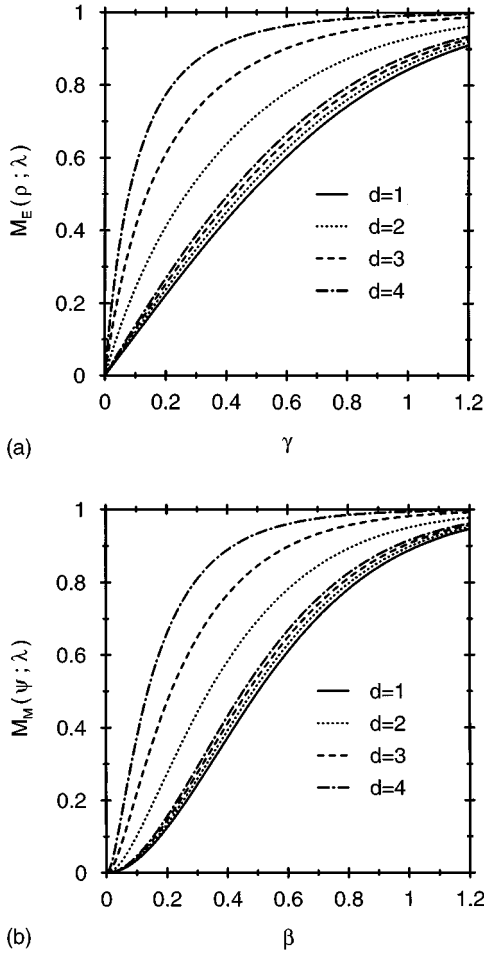
FIG. 5. End density profile $M_E(\rho;\lambda)$ as a function of $\gamma=(\rho-1)/(2\lambda^{1/2})$ (a) and monomer density profile $M_M(\psi;\lambda)$ as a function of $\beta=(\psi-1)/(2\lambda^{1/2})$ (b) of an ideal chain for $2\lambda^{1/2}=0.2$ (lower set of lines) and $2\lambda^{1/2}=5$ (upper set of lines). For $d=1$ there is no dependence on λ. Note that both densities approach their bulk values more rapidly as d increases. For the small value for λ the curves for $d=2$, 3, and 4 are close to the curve for $d=1$, which corresponds to the planar boundary.

the following we assume that the surface is purely repulsive, which is described by the Dirichlet boundary condition $c=+\infty$. It is convenient to normalize the end density with respect to its bulk value [19] and to introduce the quantity [35] [see Eq. (2.5)]

$$M_E(\rho;\lambda)\equiv\hat{\mathcal{Z}}_\lambda(\rho;\zeta=\infty)/\hat{\mathcal{Z}}_{\lambda,b}^{(D)}. \quad (3.1)$$

For $d=1$ and $d=3$ Eq. (2.15a) leads to [30]

$$M_E(\rho;\lambda)=1-\omega\,\text{erfc}\,\gamma \quad (3.2)$$

with γ defined in Eq. (2.15b), $\omega=1$ for $d=1$, and $\omega=\rho^{-1}=(1+2\lambda^{1/2}\gamma)^{-1}$ for $d=3$.

Figure 5(a) shows how M_E as a function of the scaled distance γ depends on the shape of the boundary, which is characterized by the dimension d of the radial subspace. For $d=2$ and 4 we have performed the inverse Laplace transform in Eq. (2.5) numerically. Figure 5(a) shows both the situation in which the unperturbed polymer size [20] $\mathcal{R}$ is much smaller ($2\lambda^{1/2}=0.2$) and that in which it is much

larger ($2\lambda^{1/2}=5$) than the radius R of the generalized cylinder. As expected from Eq. (2.4a), the end density increases linearly for small distances $\rho-1=(r_\perp-R)/R\ll1$ and approaches the bulk value for $\gamma\gg1$ because in this limit the chain is unlikely to reach the surface. For small $\lambda=L/R^2$ it is plausible that the surface curvature is negligible and that the curves for $d=2$, 3, and 4 should be close to the curve for $d=1$, which corresponds to the planar boundary [36]. However, if λ is large, the relative reduction $1-M_E$ of possible configurations due to the presence of the surface depends on d as expected intuitively; it is most pronounced for an infinite planar surface ($d=1$), less for a cylindrical ($d=2$), and even less for a spherical ($d=3$) surface. For this reason M_E approaches its bulk value more rapidly for larger d.

This is in line with the limit of M_E for $\lambda\to\infty$ with $\rho>1$ fixed, which equals zero for $d\leq2$ and $1-\rho^{-(d-2)}$ for $d>2$, respectively [see Eq. (2.16)]. For $d=2$ (cylinder) M_E vanishes logarithmically as $M_E\simeq(2\ln\rho)/(\ln\lambda)$ [37]. These results for $R,r_\perp\ll\mathcal{R}$ are complemented by those for $R\ll r_\perp,\mathcal{R}$, which we shall obtain within a more general framework in Sec. IV.

B. Monomer density

The monomer density at the point $\mathbf{y}=(\mathbf{y}_\perp,\mathbf{y}_\parallel)\in V$ for a solution of freely moving ideal chains is proportional [1,4] to the numerator of the rhs of Eq. (1.6) integrated over the positions $\mathbf{r}$ and $\mathbf{r}'$ of the two chain ends. Considering again a purely repulsive surface one finds for the bulk-normalized monomer density for ideal chains the expression (recall that $\hat{\mathcal{Z}}_{\lambda,b}^{(D)}=1$)

$$M_M(\psi;\lambda)=\frac{1}{\lambda}\int_0^\lambda d\lambda'\,\hat{\mathcal{Z}}_{\lambda-\lambda'}(\psi;\zeta=\infty)\hat{\mathcal{Z}}_{\lambda'}(\psi;\zeta=\infty),$$

$$(3.3)$$

in which $\psi\equiv y_\perp/R$ denotes the scaled distance from the axis of the generalized cylinder where the density is monitored.

For $d=1$ and $d=3$ we obtain the explicit results [26]

$$M_M(\psi;\lambda)=1+\frac{4\beta}{\sqrt{\pi}}[\omega\exp(-\beta^2)-\omega^2\exp(-4\beta^2)]$$

$$-2\omega(1+2\beta^2)\,\text{erfc}\,\beta+\omega^2(1+8\beta^2)\,\text{erfc}\,2\beta,$$

$$(3.4)$$

where $\beta\equiv(\psi-1)/(2\lambda^{1/2})$, $\omega=1$ for $d=1$, and $\omega=\psi^{-1}=(1+2\lambda^{1/2}\beta)^{-1}$ for $d=3$. For the planar case $d=1$ Eq. (3.4) reduces to Eq. (3.91) of Ref. [4].

Figure 5(b) shows the behavior of M_M as a function of the scaled distance β for the special cases $2\lambda^{1/2}=0.2$ and 5 and for several dimensions d of the radial subspace. The monomer density M_M increases quadratically for small distances $\psi-1\ll1$ and approaches the bulk value for $\beta\gg1$ [compare the corresponding behavior of the end density M_E discussed above in Fig. 5(a)].

C. Free energy for immersing a particle

Upon immersing a single particle $\mathcal{K}$ into a dilute polymer solution the free energy of the system changes by an amount

$$F_{\mathcal{K}} = -k_B T \ln[(Z_{L,\mathcal{V}} + \delta Z_{L,\mathcal{V}}^{(\mathcal{K})})/Z_{L,\mathcal{V}}]^{\mathcal{N}}. \qquad (3.5)$$

Here we consider a particle $\mathcal{K}$ of finite size and $\mathcal{N}$ polymer chains inside a finite volume $\mathcal{V}$. The quantity $Z_{L,\mathcal{V}}$ is the partition function of a single free polymer chain in the absence of the particle $\mathcal{K}$ and $\delta Z_{L,\mathcal{V}}^{(\mathcal{K})}$ its change due to the presence of $\mathcal{K}$. Consider now a particle $\mathcal{K}$ with the form of the sectional volume $K \cap \mathcal{V}$ between the generalized cylinder K and the finite volume $\mathcal{V} = \mathcal{V}_\| \mathcal{V}_\perp$ (where $\mathcal{V}_\|$ and $\mathcal{V}_\perp$ are the volumes of the parallel and perpendicular subspaces of $\mathcal{V}$, respectively) so that $\mathcal{K}$ will approach K as $\mathcal{V}_\| \to \infty$ [38]. In the limits $\mathcal{V}_\|, \mathcal{V}_\perp \to \infty$ the ratios

$$Z_{L,\mathcal{V}}/\mathcal{V} \to \hat{Z}_{L,b}^{(D)} \qquad (3.6a)$$

and

$$\delta Z_{L,\mathcal{V}}^{(\mathcal{K})}/\mathcal{V}_\| \to \delta Z_L^{(K)} = \int_{\mathbb{R}^d} d^d r_\perp [\hat{Z}_L(r_\perp) - \hat{Z}_{L,b}^{(D)}] \quad (3.6b)$$

are independent of $\mathcal{V}$. $\hat{Z}_L(r_\perp)$ is the partition function introduced in Eq. (2.1), which vanishes for $r_\perp < R$. Thus in the thermodynamic limit (with a finite number density $\mathcal{N}/\mathcal{V}$ of polymer chains in the bulk) one has

$$F_{\mathcal{K}}/\mathcal{V}_\| \to p_0(-\delta Z_L^{(K)})/\hat{Z}_{L,b}^{(D)} \equiv p_0 \delta f_K, \qquad (3.6c)$$

where $p_0 = k_B T \mathcal{N}/\mathcal{V}$ is the (ideal gas) pressure in the system without the particle and

$$\delta f_K = R^d \frac{\Omega_d}{d} + R^d \Omega_d \int_1^\infty d\rho \rho^{d-1}[1 - M_E(\rho; \mathcal{R}/R)]; \qquad (3.7)$$

$\Omega_d = 2\pi^{d/2}/\Gamma(d/2)$ is the surface area of the d-dimensional unit sphere. The first term in Eq. (3.7) arises from the region $0 < r_\perp < R$ in Eq. (3.6b) where $\hat{Z}_L(r_\perp)$ does not contribute.

Equations (3.6) and (3.7) apply both for a dilute solution of ideal chains and for chains with excluded volume interaction [35]. This is indicated in Eq. (3.7) by using the argument $\mathcal{R}/R$ in M_E instead of λ as in Eq. (3.1). For ideal chains one can use the explicit expression (2.4a) for $\mathcal{X}$ and finds

$$\int_1^\infty d\rho \rho^{d-1}[1 - M_E(\rho; \lambda)] = \mathcal{L}_{\tau \to \lambda} \left\{ \frac{K_{\alpha+1}(\sqrt{\tau})}{\tau^{3/2} K_\alpha(\sqrt{\tau})} \right\}. \qquad (3.8)$$

For short ideal chains, i.e., $\lambda = L/R^2 \ll 1$ this leads to

$$\delta f_K = R^d \frac{\Omega_d}{d} + R^{d-1} \Omega_d \left\{ \frac{2}{\sqrt{\pi}} L^{1/2} + \frac{d-1}{2} \frac{L}{R} + \frac{(d-1)(d-3)}{6\sqrt{\pi}} \frac{L^{3/2}}{R^2} + \cdots \right\}. \qquad (3.9)$$

We note that $p_0(2/\sqrt{\pi})L^{1/2}$ is the surface free energy per unit surface area for an ideal polymer solution in a half space with a *planar* boundary [38] caused by the depletion layer. While this is reflected [39] by the first term in curly brackets in Eq. (3.9), the second term in curly brackets is the first-order correction due to the surface *curvature* and represents an additional *positive* [40] contribution to the free energy for the exterior of a cylinder ($d=2$) and a sphere ($d=3$) in three-dimensional space. In Appendix C we generalize the small-curvature expansion (3.9) to more general particle shapes.

The result (3.9) can be compared with an approximation in which the interaction between the particle K and the polymer chain is as if the polymer chain would be a pointlike hard sphere (PHS) [41] of radius $\widetilde{\mathcal{R}} \equiv (2/\sqrt{\pi})L^{1/2}$; otherwise the chains are treated as pointlike objects without mutual interaction. Within this PHS approximation the counterpart of δf_K is given by

$$\delta f_K^{(\text{PHS})} = (R + \widetilde{\mathcal{R}})^d \frac{\Omega_d}{d} = R^d \frac{\Omega_d}{d} + R^{d-1} \Omega_d \left\{ \widetilde{\mathcal{R}} + \frac{d-1}{2} \frac{\widetilde{\mathcal{R}}^2}{R} + \frac{(d-1)(d-2)}{6} \frac{\widetilde{\mathcal{R}}^3}{R^2} + \cdots + \frac{1}{d} \frac{\widetilde{\mathcal{R}}^d}{R^{d-1}} \right\}. \qquad (3.10)$$

This series terminates for integer values of d. Note that the prefactor in the relation between $\widetilde{\mathcal{R}}$ and $L^{1/2}$ has been chosen such that for a plate ($d=1$) [38] one has $\delta f_K^{(\text{PHS})} = \delta f_K$. Thus, apart from a numerical prefactor of order unity in front of the third term, Eq. (3.10) reproduces correctly the three leading terms in Eq. (3.9). However, it does not reproduce the dependence $\propto(d-3)$ of the fourth term in Eq. (3.9), which is quadratic in the curvature.

In the opposite limit $L/R^2 \gg 1$ the phs approximation fails completely. In order to demonstrate this we consider a *sphere* ($D = d = 3$) for which Eqs. (3.7) and (3.8) lead to [38]

$$\delta f_{\text{sphere}} = 4\pi R^3 \left\{ \frac{1}{3} + \frac{2}{\sqrt{\pi}} \frac{L^{1/2}}{R} + \frac{L}{R^2} \right\}, \qquad (3.11)$$

which applies for arbitrary $\lambda = L/R^2$ and is consistent with Eq. (3.9). Thus, for $\lambda \gg 1$ one has $\delta f_{\text{sphere}} \sim \lambda$, which is much smaller than the phs approximation ($\sim \lambda^{3/2}$) would predict [42]. This is expected because the chain will deform and coil around the spherical particle and its partition function will be less reduced than in the phs approximation.

Meijer and Frenkel [14] have introduced an effective polymer radius $\widetilde{\mathcal{R}}_{\text{eff}}(\mathcal{R}, R)$ which follows from equating
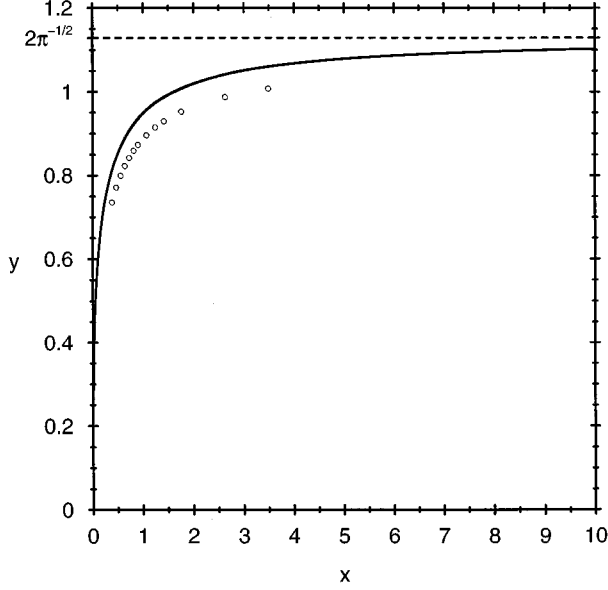
FIG. 6. Comparison of our result for $\delta f_{\mathrm{sphere}}$ with simulation data obtained by Meijer and Frenkel [14]. The figure displays the function $\widetilde{\mathcal{R}}_{\mathrm{eff}}(\mathcal{R},R)$ defined by $\delta f_{\mathrm{sphere}}^{(\mathrm{PHS})}(R;\widetilde{\mathcal{R}}\equiv\widetilde{\mathcal{R}}_{\mathrm{eff}})$ $=\delta f_{\mathrm{sphere}}(R;L=\mathcal{R}^2/6)$ where $\delta f_{\mathrm{sphere}}^{(\mathrm{PHS})}$ and $\delta f_{\mathrm{sphere}}$ are given by Eq. (3.10) with $d=3$ and by Eq. (3.11), respectively, using the reduced variables $x=R/\mathcal{R}_{\mathrm{gyr}}$ and $y=\widetilde{\mathcal{R}}_{\mathrm{eff}}/\mathcal{R}_{\mathrm{gyr}}$ (see the main text). Our result (3.11) implies the explicit form $x^2(y-2\pi^{-1/2})+x(y^2-1)+y^3/3=0$, which is shown as the solid line. The open circles are taken from Fig. 2 of Ref. [14]. Note the strong deviation for long chains ($x\ll1$) from the behavior $y\simeq2\pi^{-1/2}$ (dashed line) valid for short chains ($x\gg1$).

$\delta f_{\mathrm{sphere}}^{(\mathrm{PHS})}$ with $\delta f_{\mathrm{sphere}}$. Figure 6 shows a comparison between their simulation data and our analytical result (3.11). We choose their variables

$$x=R/L^{1/2}=\sqrt{6}R/\mathcal{R}=R/\mathcal{R}_{\mathrm{gyr}} \qquad (3.12\mathrm{a})$$

and

$$y=\widetilde{\mathcal{R}}_{\mathrm{eff}}/L^{1/2}=\sqrt{6}\widetilde{\mathcal{R}}_{\mathrm{eff}}/\mathcal{R}=\widetilde{\mathcal{R}}_{\mathrm{eff}}/\mathcal{R}_{\mathrm{gyr}}, \qquad (3.12\mathrm{b})$$

where $\mathcal{R}_{\mathrm{gyr}}$ is the radius of gyration [16]. The deviation is only about 5% and is expected to disappear if the number of links of the chain and the sphere radius in the simulation are sufficiently large. One should note the crossover from the behavior $\widetilde{\mathcal{R}}_{\mathrm{eff}}\simeq\mathcal{R}=(2/\sqrt{\pi})L^{1/2}$ (i.e., $y\simeq2/\sqrt{\pi}$) for short chains $x\gg1$ to the behavior $\widetilde{\mathcal{R}}_{\mathrm{eff}}\simeq(3RL)^{1/3}$ [i.e., $y\simeq(3x)^{1/3}$] for long chains $x\ll1$. Both limits of the crossover follow immediately from Eqs. (3.10) and (3.11).
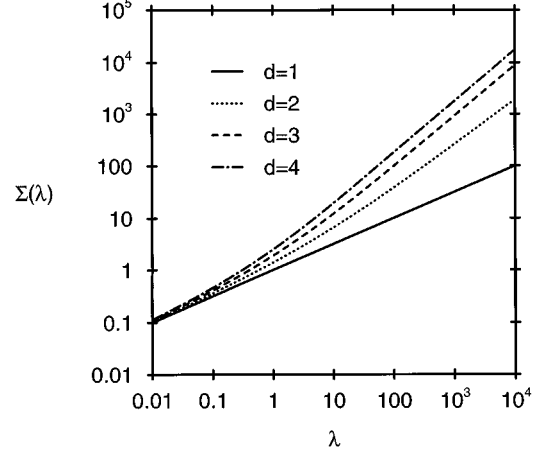

FIG. 7. Crossover function $\Sigma(\lambda)$ for the configurational free energy for immersing a particle for several dimensions d of the radial subspace. The linear behavior $\Sigma(\lambda\to\infty)\simeq[(d-2)/2]\pi^{1/2}\lambda$ valid for $d=3,4$ corresponds to the expansion (4.14) for small particle radii.

Figure 7 shows the behavior of δf_K for several dimensions d of the radial subspace in terms of the function

$$\Sigma(\lambda)\equiv\frac{1}{2}\sqrt{\pi}\left[\frac{\delta f_K}{R^d\Omega_d}-\frac{1}{d}\right]. \qquad (3.13)$$

The prefactor has been chosen such that $\Sigma(\lambda)=\lambda^{1/2}$ for $d=1$. According to Eqs. (3.13) and (3.7) the function $\Sigma(\lambda)$ is essentially given by the integral in Eq. (3.8) over the relative reduction $1-M_E(\rho)$ of chain configurations with one end fixed. Note that although $1-M_E$ is largest for a planar boundary ($d=1$) and decreases for larger $d=2$, 3, and 4 [compare Fig. 5(a)], the behavior of $\Sigma(\lambda)$ is opposite [43]: Σ is *smallest* for the planar boundary case $d=1$ and *increases* for $d=2$, 3, and 4. This effect is caused by the prefactor ρ^{d-1} in the integrand on the left-hand side (lhs) of Eq. (3.8), i.e., the relevant integration volume, which becomes larger as d increases. Compare also the explicit behavior of $\Sigma(\lambda\to\infty)$ for $d>2$ presented at the end of Sec. IV C below.

IV. EXPANSION FOR SMALL RADII

In the limit for which the radius R of the generalized cylinder K is much smaller [44] than the length scales set by the polymer end-to-end distance $\mathcal{R}$ and the distances $r_\perp-R$ or $y_\perp-R$ from the surface for which the densities M_E or M_M are monitored, one may use an expansion introduced in Ref. [17]. There it was argued that for a field theory such as (1.5) the statistical weight $e^{-\Delta\mathcal{H}_K}$, which describes the presence of K can, for $c=+\infty$, be replaced by

$$e^{-\Delta\mathcal{H}_K}\propto1+\mathcal{A}_KR^{x_K}\times\left\{\begin{array}{ll}\int_{\mathbb{R}^\delta}d^\delta y_\parallel\ \Phi^2(\mathbf{y}_\perp=0,\mathbf{y}_\parallel)+\cdots, & \delta>0, \\[2ex] \Phi^2(\mathbf{y}=0)+\cdots, & \delta=0.\end{array}\right. \qquad (4.1)$$

In the upper line the integration over the cylinder axis in Ref. [17(b)] has been generalized to a $\delta = (D-d)$-dimensional integration over the ''axis'' of the generalized cylinder K. The quantity $\mathcal{A}_K$ is an amplitude (see below). The leading nontrivial dependence on R is determined by the exponent

$$x_K = x_{\Phi^2} - \delta, \tag{4.2a}$$

where x_{Φ^2} is the *bulk* scaling dimension of the ''energy density'' Φ^2. The ellipses in Eq. (4.1) denote contributions that are of higher order in R. For the Gaussian model $x_{\Phi^2} = D-2$ and thus in this case

$$x_K = d-2 = 2\alpha \tag{4.2b}$$

depends on d but not on D. The expansion (4.1) makes sense only for $x_K > 0$, i.e., in the case of the Gaussian model for $d > 2$ [see, however, Eq. (4.10) below]. This has important consequences for the polymer statistics near a purely repulsive generalized cylinder as we shall demonstrate in the following.

A. End density

Using Eq. (4.1) together with the definition of M_E in Eq. (3.1) one finds

$$M_E \simeq 1 + \mathcal{A}_K R^{x_K} 2 L g_E(r_\perp, L), \tag{4.3a}$$

where

$$g_E(r_\perp, L) = \begin{cases} \int_{\mathbb{R}^\delta} d^\delta y_\parallel \, \hat{m}_b(\mathbf{y}_\perp = 0, \mathbf{y}_\parallel ; \mathbf{r}; L), & \delta > 0, \\ \hat{m}_b(\mathbf{y} = 0; \mathbf{r}; L), & \delta = 0. \end{cases} \tag{4.3b}$$

The R-independent quantity

$$\hat{m}_b(\mathbf{y}; \mathbf{r}; L) = \hat{m}_b(|\mathbf{y} - \mathbf{r}|; L)$$

$$= \frac{1}{L} \mathcal{L}_{t \to L} \int_{\mathbb{R}^D} d^D r' \langle \Phi(\mathbf{r}) \Phi(\mathbf{r}') \tfrac{1}{2} \Phi^2(\mathbf{y}) \rangle_b$$

$$\times \left[\mathcal{L}_{t \to L} \int_{\mathbb{R}^D} d^D r' \langle \Phi(\mathbf{r}) \Phi(\mathbf{r}') \rangle_b \right]^{-1}, \tag{4.3c}$$

with $\langle \rangle_b$ denoting thermal averages in the unbounded bulk space, is the monomer fraction density at $\mathbf{y} = (\mathbf{y}_\perp, \mathbf{y}_\parallel) \in \mathbb{R}^D$ for a single chain in the unbounded bulk with one end fixed at $\mathbf{r} \in \mathbb{R}^D$ and the other end free. Similarly as $m(\mathbf{y})$ in Eq. (1.6) it is normalized: $\int_{\mathbb{R}^D} d^D y \, \hat{m}_b(|\mathbf{y} - \mathbf{r}|) = 1$.

For an ideal chain (i.e., within a Gaussian model for Φ) we obtain

$$g_E(r_\perp, L) = \frac{1}{L} \int_0^L dL' Z_{L',b}^{(d)}(r_\perp) = \frac{1}{4\pi^{d/2}} \frac{r_\perp^{-2\alpha}}{L} \Gamma(\alpha, \eta^2) \tag{4.4a}$$

with

$$\eta = r_\perp/(2L^{1/2}), \tag{4.4b}$$

where $Z_{L,b}^{(d)}$ is the Gaussian partition function in the d-dimensional bulk space [19], and $\Gamma(\alpha, x)$ the incomplete Γ function [25]. Here we have used the relation

$$\int_{\mathbb{R}^\delta} d^\delta y_\parallel Z_{L,b}^{(D)}(|\mathbf{r} - \mathbf{y}|) = Z_{L,b}^{(d)}(|\mathbf{r}_\perp - \mathbf{y}_\perp|), \tag{4.5}$$

which implies that for an ideal chain g_E depends on d but not on D. Since M_E has the same property, this must also hold for the amplitude $\mathcal{A}_K$ in Eq. (4.3a) so that we can use the results for $D = d$ from Ref. [17(b)] in order to obtain

$$\mathcal{A}_K = -2\pi^{d/2}/\Gamma(\alpha). \tag{4.6}$$

Due to Eqs. (4.3), (4.4), and (4.6) one thus has for ideal chains

$$M_E \simeq 1 - \left(\frac{R}{r_\perp} \right)^{d-2} \Gamma(\alpha, \eta^2)/\Gamma(\alpha). \tag{4.7}$$

This result can be verified directly by using the explicit expression (2.4a) for $\mathcal{X}$ in the case $\zeta = +\infty$ and its behavior for $R \to 0$.

We expect that the relationship (4.3) is valid also for chains with EVI [45]. However, in this case one has $x_K = d - \nu^{-1}$ with the Flory exponent $\nu = \nu(D)$ [1] and one is led to consider an amplitude $\widetilde{\mathcal{A}}_K$ defined by

$$\mathcal{A}_K = \widetilde{\mathcal{A}}_K(D, d) \mathcal{R}^{1/\nu}/(2LD), \tag{4.8}$$

where $\mathcal{R}$ is the root-mean-square end-to-end distance of a single chain with EVI in the unbounded bulk (compare Refs. [20] and [35]). While due to $\nu^{-1} \neq 2$ the amplitude $\mathcal{A}_K$ is not dimensionless and depends upon details of EVI, the amplitude $\widetilde{\mathcal{A}}_K$ is *dimensionless and universal* [46]. We note that in the presence of EVI the universal function [18]

$$\mathcal{R}^D \hat{m}_b(|\mathbf{y} - \mathbf{r}|; L) \equiv M_b(|\mathbf{y} - \mathbf{r}|/\mathcal{R}) \tag{4.9a}$$

depends on D while $\widetilde{A}_K$ and

$$\mathcal{R}^d g_E(r_\perp, L) \equiv G_E(r_\perp/\mathcal{R}) \tag{4.9b}$$

in general depend on both D and d. Furthermore we expect that for $D = 3$ and in the presence of EVI the behaviors (4.1) and (4.3) apply not only for a sphere ($d = 3$) but also for a cylinder ($d = 2$) because the exponent [47(b)]

$$x_K(D = 3, d = 2) = 2 - \nu^{-1}(D = 3) \approx 0.30 \tag{4.10}$$

is *positive* in this case [whereas $x_K(d = 2) = 0$ for an ideal chain].

A simple and general result follows for $R \ll r_\perp \ll \mathcal{R}$ in which case the behavior of $\hat{m}_b(|\mathbf{y} - \mathbf{r}|)$ in Eq. (4.3c) is determined by the leading term in the short distance expansion in the unbounded bulk [47]:

$$\Phi(\mathbf{r}) \Phi^2(\mathbf{y}) = \frac{\mathcal{B}_b}{|\mathbf{r} - \mathbf{y}|^{D - (1/\nu)}} \Phi(\mathbf{r}) + \cdots, \tag{4.11a}$$

where

$$\mathcal{B}_b = \widetilde{\mathcal{B}}_b(D) 2LD/\mathcal{R}^{1/\nu}, \qquad (4.11b)$$

with a dimensionless and universal [46] bulk amplitude $\widetilde{\mathcal{B}}_b$, which depends on D. Inserting Eq. (4.11) into Eq. (4.3c) leads to [48]

$$M_E - 1 \simeq \widetilde{\mathcal{A}}_K(D,d) \widetilde{\mathcal{B}}_b(D) \mathcal{C}_K \left(\frac{R}{r_\perp}\right)^{x_K}, \qquad (4.12a)$$

where

$$\mathcal{C}_K = \begin{cases} \pi^{\delta/2} \Gamma(x_K/2)/\Gamma\left(\dfrac{D-\nu^{-1}}{2}\right), & \delta > 0 \\[2ex] 1, & \delta = 0. \end{cases} \qquad (4.12b)$$

The first line in Eq. (4.12b) follows from the integral $\int_{\mathbb{R}^\delta} d^\delta y_\parallel (r_\perp^2 + y_\parallel^2)^{-(D-\nu^{-1})/2}$, which is convergent for $x_K > 0$. The rhs of Eq. (4.12a) does not depend on $\mathcal{R}$ and suggests that in the presence of EVI M_E remains nonzero for $\mathcal{R} \to \infty$ not only for a sphere but also for a cylinder in $D = 3$. This should be compared with the ideal chain behavior for $d = 2$ where $M_E \to 0$ for $\mathcal{R} \to \infty$ as discussed in the last paragraph in Sec. III A.

B. Monomer density

The expansion (4.1) can be used to express the behavior of the monomer density M_M for small R in terms of the monomer density correlation function of a single chain in the unbounded bulk [which is related to the "magnetic" correlation function $\langle \Phi(\mathbf{r}) \Phi(\mathbf{r}') \Phi^2(\mathbf{y}) \Phi^2(\mathbf{y}') \rangle_b$]. Here we only present the explicit result for ideal chains. We find from Eqs. (3.3) and (2.4a) for $d > 2$

$$M_M \simeq 1 - \left(\frac{R}{y_\perp}\right)^{d-2} \frac{2}{\Gamma(\alpha)} \phi^{\alpha-1}$$
$$\times \exp(-\phi^2/2) W_{\alpha/2-3/2, \alpha/2}(\phi^2), \qquad (4.13a)$$

where $\phi = y_\perp/(2L^{1/2})$ and $W_{\beta,\mu}$ is Whittaker's function [25]. For $d = 3$ it reduces to

$$M_M \simeq 1 - \frac{R}{y_\perp} [2(1+2\phi^2) \operatorname{erfc}\phi - (4/\sqrt{\pi})\phi \exp(-\phi^2)],$$
$$d = 3, \quad (4.13b)$$

and for $d = 4$ to

$$M_M \simeq 1 - \left(\frac{R}{y_\perp}\right)^2 2E_2(\phi^2), \quad d = 4, \qquad (4.13c)$$

where E_2 is the exponential integral [25].

C. Free energy for the immersion of a particle

The expansion (4.1) can also be used to evaluate the behavior of the free energy $F_\mathcal{K}$ for small R upon immersing a particle $\mathcal{K} \equiv K$ into a dilute polymer solution as discussed in Sec. III C. For $R \ll \mathcal{R}$ the integral in Eq. (3.7) is dominated by the region $R \ll r_\perp = \mathcal{O}(\mathcal{R})$ where Eq. (4.3) holds. Since

$\int_{\mathbb{R}^d} d^d r_\perp g_E = 1$ one finds with Eq. (4.8) that the quantity δf_K in Eq. (3.7) for $R \ll \mathcal{R}$ tends to

$$\delta f_K \to \delta \widetilde{f}_K = -\mathcal{A}_K 2LR^{x_K} = -R^d \frac{\widetilde{\mathcal{A}}_K}{D} \left(\frac{\mathcal{R}}{R}\right)^{1/\nu}. \qquad (4.14)$$

This relation applies for both ideal chains and chains with EVI as long as $x_K > 0$. For ideal chains and $d > 2$ it can be verified by using Eqs. (3.8) and (4.6). For the function $\Sigma(\lambda)$ in Eq. (3.13) it leads to the asymptotic behavior $\Sigma(\lambda \to \infty) \simeq [(d-2)/2] \sqrt{\pi} \lambda$, which increases with d in accordance with Fig. 7.

D. Effective interaction of a particle with a planar wall

In the following we consider a particle $\mathcal{K}$ immersed in a dilute polymer solution that fills a half space (HS) bounded by a planar wall W. The effective interaction of this particle with the wall W is given by the difference of the free energy for immersing a particle at a finite and an infinite distance, respectively, from the wall:

$$\delta F_{\mathcal{K},W} = (F_{\mathcal{K},W} - F_W) - F_\mathcal{K}. \qquad (4.15)$$

If $\mathcal{K}$ approaches a generalized cylinder K with its axis parallel to and a distance a apart from the planar wall the interaction free energy per "unit axis length" [38] $\delta F_{\mathcal{K},W}/\mathcal{V}_\parallel$ remains finite. $F_\mathcal{K}/\mathcal{V}_\parallel$ approaches the rhs of Eq. (3.6c); the thermodynamic limit of $(F_{\mathcal{K},W} - F_W)/\mathcal{V}_\parallel$ has the same form as the rhs of Eq. (3.6c) with $\delta Z_L^{(K)}$ replaced by

$$\delta Z_L^{(K,W)} = \int_{\mathbb{R}^\delta} d^\delta r_\parallel \int_{HS_0} d^d r_\perp \int_{HS_0} d^d r_\perp' [Z_L^{(K,W)}(\mathbf{r}, \mathbf{r}')$$
$$- Z_L^{(W)}(\mathbf{r}, \mathbf{r}')]. \qquad (4.16)$$

Here $Z_L^{(K,W)}$ and $Z_L^{(W)}$ denote partition functions of a chain with two ends fixed, which coils in the half space

$$\text{HS} = \{\mathbf{r} = (r_{\perp 1}, r_{\perp 2}, \ldots, r_{\perp d}; \mathbf{r}_\parallel) \in \mathbb{R}^d \times \mathbb{R}^\delta; r_{\perp 1} > -a\}$$
$$(4.17a)$$

bounded by the wall W at $r_{\perp 1} = -a$ in the presence and absence, respectively, of the generalized cylinder K with axis at $\mathbf{r}_\perp = 0$ and radius R. The integrations over $\mathbf{r}_\perp$ and $\mathbf{r}_\perp'$ in Eq. (4.16) are over the subspace HS_0 of HS where $\mathbf{r}_\parallel = 0$ in Eq. (4.17a). It is understood that $a \geq R$ and that $Z_L^{(K,W)}$ vanishes for $r_\perp < R$ or $r_\perp' < R$. In Eq. (4.16) there is no integration over $\mathbf{r}_\parallel'$ since both $Z_L^{(K,W)}$ and $Z_L^{(W)}$ depend on $\mathbf{r}_\parallel$ and $\mathbf{r}_\parallel'$ only in the form $|\mathbf{r}_\parallel - \mathbf{r}_\parallel'|$ and because $\mathcal{V}_\parallel$ has been factored out. For later use we introduce another coordinate representation

$$\text{HS} = \{\mathbf{x} = (z, \mathbf{s}) \in \mathbb{R} \times \mathbb{R}^{D-1}; z > 0\} \qquad (4.17b)$$

for the HS in Eq. (4.17a) where

$$z = r_{\perp 1} + a \qquad (4.17c)$$

is the distance from the boundary wall W and

$$\mathbf{s} = (r_{\perp 2}, \ldots, r_{\perp d}; \mathbf{r}_\parallel) \qquad (4.17d)$$

comprises the $D - 1$ components parallel to W.

The finite limit $\delta f_{K,W}$ of $\delta F_{\mathcal{K},W}/(\mathcal{V}_{\parallel}p_0)$ as $\mathcal{K} \to K$ [38] is the counterpart of δf_K in Eq. (3.6c) and depends only on the radius R, the polymer end-to-end distance $\mathcal{R}$, and the distance a of the axis of the generalized cylinder from the wall [18]. While the full function $\delta f_{K,W}$ is not known exactly in general even for a Gaussian chain, one finds a simple explicit form in the limit $R \ll \mathcal{R}, a$. In this case the expansion (4.1) can be used to evaluate Eq. (4.16), which leads to a dependence of $\delta f_{K,W}$ on a proportional to the bulk-normalized monomer density $M_M^{(W)}$ in a half space, which has the form [4]

$$M_M^{(W)}(a/\mathcal{R}) \propto \mathcal{L}_{t \to L} \int_{\mathrm{HS}} d^D x \int_{\mathrm{HS}} d^D x'$$
$$\times \left\langle \Phi(\mathbf{x}) \Phi(\mathbf{x}') \frac{1}{2} \Phi^2(a, \mathbf{s}=0) \right\rangle_{\mathrm{hs}} . \quad (4.18)$$

Here $\langle \rangle_{\mathrm{hs}}$ denotes the thermal average for the half space [49] with the wall at $z=0$ [see Eq. (4.17b)]. Since the contribution to $\delta f_{K,W}$ from $-F_{\mathcal{K}}$ in Eq. (4.15) is given by $-\delta f_K$ and since $\delta f_{K,W}$ must vanish in the limit $a \to \infty$ we obtain for $R \ll \mathcal{R}, a$,

$$\delta f_{K,W} \simeq \delta \widetilde{f}_K [M_M^{(W)}(a/\mathcal{R}) - 1], \quad (4.19)$$

with $\delta \widetilde{f}_K$ defined in Eq. (4.14). This means that the presence of the polymer chains leads to an *increase* of $\delta f_{K,W}$ for increasing a and thus to an *attractive* force between the wall and the particle. In the particular case $R \ll a \ll \mathcal{R}$ one has $\delta f_{K,W} \simeq -\delta \widetilde{f}_K$ because in this limit $M_M^{(W)}$ vanishes [1] as $(a/\mathcal{R})^{1/\nu}$. Equations (4.18) and (4.19) hold for both ideal chains and chains with EVI. For ideal chains $M_M^{(W)}$ corresponds to the quantity in Eq. (3.4) for $d=1$.

The general mechanism for the attractive depletion interaction has first been pointed out by Asakura and Oosawa [41]. This interaction is relevant for colloids (see, e.g., the classic experiments of Sperry, Hopfenberg, and Thomas [50], the recent reviews in Ref. [51], and the references cited therein). While approximate expressions for the interaction exist for the case $\mathcal{R} \ll R$ [6,7] and for $\mathcal{R}$ of the order of R [14], to our knowledge Eq. (4.19) is the first quantitative result for the case $\mathcal{R} \gg R$.

Similar results can be obtained for the solvation force between two spherical particles or between a sphere and a cylinder in unbounded space with radii that are much smaller than both $\mathcal{R}$ and their mutual distance a. In these cases the dependence on $a/\mathcal{R}$ is determined by the monomer density correlation function of a single chain in unbounded bulk. For three or more spherical particles with small radii the expansion (4.1) leads to higher monomer correlation functions of a single chain and to a polymer-induced interaction that is not pairwise additive [14] (compare the discussion in Ref. [17] for the corresponding situation of binary liquid mixtures at criticality).

V. CONCLUDING REMARKS AND SUMMARY

We have investigated the interaction of a long flexible polymer chain with rigid particles of spherical or cylindrical shape [52]. Possible applications include colloidal particles of spherical or rodlike shape [7,8,50,51] immersed into a dilute polymer solution. We have studied both the case in which the surface of the particles is purely repulsive for the chain monomers (depletion case) and the case of a surface with a short-ranged attraction, which leads to the possibility of an adsorption-desorption transition. While for the latter case explicit results have been obtained only for *ideal* chains, for the depletion case we have considered both ideal chains and chains with an EVI.

We have used the polymer-magnet analogy (PMA) [1,16,4], which relates the chain problem to properties of a field theory. As discussed in Sec. I, the field theory corresponding to an ideal chain is characterized by the Hamiltonian (1.5). In the presence of EVI one may use a similar field theory in which, however, the order parameter $\mathbf{\Phi} \equiv (\Phi_1, \ldots, \Phi_N)$ has N components and $\mathcal{H}_K$ in Eq. (1.5) is to be supplemented by an interaction $\propto \int_V d^D r |\mathbf{\Phi}|^4$.

The PMA is already useful for an ideal chain. The propagator G of the Gaussian field theory (1.5) is known explicitly (Appendix B) for an arbitrary value of the surface parameter c. The chain partition function Z_L follows by a Laplace transform [see Eq. (1.4) and Sec. II A]. This approach allows one to obtain the *full* partition function for an ideal chain near the adsorption-desorption transition, which contains contributions from both the ground state [53] and excited states. The renormalization-group approach, which is well advanced for such local field theories, leads via the PMA to an explanation of universality and scaling in polymer statistics [1,4,16]. In combination with perturbative methods such as the ε expansion [16] the influence of EVI can be studied systematically and quantitatively.

In addition short-distance expansions [1,4,16,47] (SDE) for such field theories offer important nonperturbative insights into the polymer statistics. Interesting features of polymer solutions that are exposed to immersed spherical or cylindrical objects of finite extension (i.e., particle radius R) can be inferred from the special type [17] of SDE discussed in Sec. IV. We have shown how to use this expansion in order to obtain results for polymers in the depletion case if the particle radius R is much smaller than the (root-mean-square) end-to-end distance $\mathcal{R}$ of a chain in the bulk polymer solution.

Still another type of SDE applies for a ''small'' distance from a planar surface [22]. This is modified in an interesting way if the surface is curved. Consider, e.g., the Gaussian model (1.5) for $c = +\infty$. In this case Eq. (B3) implies that the propagator $G = G(r_\perp, r'_\perp, \vartheta, |\mathbf{r}_\parallel - \mathbf{r}'_\parallel|; t, c = \infty, R)$ reduces to

$$G(r_\perp \searrow R) = \mathcal{D} \frac{\partial G}{\partial r_\perp}\Big|_{r_\perp = R} + O((r_\perp - R)^3) \quad (5.1a)$$

if the other variables are kept fixed and

$$\mathcal{D}(r_\perp) = (r_\perp - R)\left[1 - \frac{d-1}{2} \frac{r_\perp - R}{R}\right]; \quad (5.1b)$$

TABLE I. End density M_E for $\mathcal{R} \to \infty$ and various geometries in $D=3$ spatial dimensions. While the result for a sphere and a cylinder in the first line apply for $R, r_\perp \ll \mathcal{R}$ with arbitrary $R/r_\perp < 1$, those in the second line apply only for $R \ll r_\perp \ll \mathcal{R}$. The variable z for the half space denotes the distance from the planar wall. The exponents 1.30 and 0.30 equal $d - \nu^{-1}$ with $d=3$ and $d=2$, respectively, and with $\nu^{-1} \approx 1.70$ [47(b)]. The exponent 0.82 for the half space is a critical surface exponent; a and b are universal amplitudes. For a small distance from the surface of a sphere and a cylinder ($r_\perp - R \ll R, \mathcal{R}$) we expect a power-law dependence $M_E \sim (r_\perp - R)^{0.82}$ with the same surface exponent as for a planar surface.

	Free space	Sphere	Cylinder	Half space
Ideal chains	1	$1 - R/r_\perp$	$\sim \ln(r_\perp/R)/\ln(\mathcal{R}/R)$	$\sim z/\mathcal{R}$
Chains with EVI	1	$1 - a(R/r_\perp)^{1.30}$	$1 - b(R/r_\perp)^{0.30}$	$\sim (z/\mathcal{R})^{0.82}$

the term $\propto (r_\perp - R)^2$, which is of second order in the small distance from the surface, is due to the curvature and drops out for $1/R \to 0$ [54]. The short-distance dependence $\mathcal{D}$ is proliferated to the partition function Z_L in Eq. (1.4) and to integrated quantities such as χ in Eq. (2.2) and $\hat{Z}_L$ in Eq. (2.1):

$$\chi(r_\perp \searrow R) = \mathcal{D} \left. \frac{\partial \chi}{\partial r_\perp} \right|_{r_\perp = R} - \frac{1}{2}(r_\perp - R)^2 + O((r_\perp - R)^3)$$

(5.2)

and

$$\hat{Z}_L(r_\perp \searrow R) = \mathcal{D} \left. \frac{\partial \hat{Z}_L}{\partial r_\perp} \right|_{r_\perp = R} + O((r_\perp - R)^3). \quad (5.3)$$

The second term on the rhs of Eq. (5.2) appears already for a planar surface and arises from those contributions to the integral in Eq. (2.2) where $r_\perp'$ is close to the surface $r_\perp' = R$ [55]. Since it does not depend on t it drops out from the inverse Laplace transform and is absent in Eq. (5.3).

In the following we summarize our main results, starting with the depletion phenomena in which a dilute polymer solution is in contact with one (or more) purely repulsive particles.

(1) For a single sphere or cylinder both the density of chain ends M_E and the monomer number density M_M in the surrounding polymer solution have been considered as a function of the distance $r_\perp - R$ from the particle surface and of the ratio $\mathcal{R}/R$ of the polymer end-to-end distance $\mathcal{R}$ and the particle radius R. For ideal chains the explicit results are shown in Figs. 5(a) and 5(b). We have found analytic expressions [see Eqs. (4.7) and (4.13)] for $R \ll r_\perp, \mathcal{R}$ with $r_\perp/\mathcal{R}$ arbitrary and for $R, r_\perp \ll \mathcal{R}$ with arbitrary $R/r_\perp < 1$ (see the last paragraph in Sec. III A). If the shape of the boundary changes from a plane via a cylinder to a sphere the depletion hole in M_E and M_M becomes less and less pronounced if $\mathcal{R} \gg R$ while for $\mathcal{R} \ll R$ the profiles are close to those for a planar boundary. The quantitative behavior of M_E for $\mathcal{R} \to \infty$ is given for these three cases in the first line of Table I. For chains with EVI we have obtained the behavior of M_E for spheres and cylinders in the region $R \ll r_\perp \ll \mathcal{R}$ [see Eq. (4.12)]. This is shown in the second line of Table I. We emphasize that the EVI weakens the repulsive character of the boundaries. In particular for the cylinder it leads to a finite limit of M_E for $\mathcal{R} \to \infty$.

(2) The free energy from conformation changes upon immersing a single particle into a dilute polymer solution can be expressed in terms of M_E [see Eq. (3.7)] and depends on $\mathcal{R}/R$. For ideal chains we have evaluated the complete dependence for spheres and cylinders (see Fig. 7). Recent simulation data for a sphere [14] are very close to our exact asymptotic result (see Fig. 6). In the limit $\mathcal{R} \gg R$ we have found a general expression for this free energy difference [see Eq. (4.14)], which is also valid in the presence of EVI. Bounding surfaces of more general shapes such as those of flexible membranes with a small but spatially varying local curvature have also been addressed (see Appendix C).

(3) If a particle is positioned near the planar container wall of a dilute polymer solution the interference between the depletion in front of the wall and around the particle leads to an effective interaction between the wall and the particle. In the particular case in which the radius R of the particle is much smaller than both the distance a of the particle from the wall and the end-to-end distance $\mathcal{R}$ in the polymer solution the interaction free energy is determined by the monomer density $M_M^{(W)}$ in the half space and is given by Eq. (4.19). Such effective interactions are experimentally relevant [50,51].

We now summarize our results for a single ideal polymer chain, which is fixed with one end near a curved boundary endowed with an *attractive* short-ranged surface potential.

(4) The ''magnetic'' phase diagram and the corresponding phase diagram for polymer adsorption have been discussed for the Gaussian (ideal chain) case. Figure 2(a) shows the ''magnetic'' phase diagram as a function of the parameters $\zeta = cR$ and $\tau = tR^2$, which occur in the Hamiltonian (1.5) of the Gaussian field theory. The quantity c is an inverse extrapolation length and characterizes the short-ranged surface potential [compare Eq. (1.2c) and Appendix A]. The ''magnetic'' phase diagram translates into a phase diagram for polymer adsorption shown in Fig. 2(b) in which the parameter τ is replaced by $\lambda^{-1} = \mathcal{R}^2/L$ and the ''chain length'' L is related to the end-to-end distance $\mathcal{R}$ via $\mathcal{R}^2 = 2LD$ [20]. In the limit of an infinite chain length ($\lambda^{-1} = 0$) important properties change nonanalytically as ζ passes ζ^*. In particular the fraction of chain monomers in a layer of finite width around the surface vanishes for $\zeta > \zeta^*$ (nonadsorbed state) while it is finite for $\zeta < \zeta^*$ (adsorbed state). (The effects of EVI on the results obtained for an ideal chain will be addressed below.)

(5) For an infinite ideal chain in the adsorbed state ($\lambda^{-1} = 0, \zeta < \zeta^*$) the layer density $P(c,R)$ of the monomer fraction near the surface and the ''decay length'' $a_\perp$, which is a quantitative measure of the thickness of the adsorption layer, are shown in Figs. 3(a) and 3(b) as a function of the

scaled increment $|\zeta - \zeta^*|$ of the surface parameter c. In particular for $d=2$ (cylinder) the fraction density P vanishes exponentially [11,33] for $\zeta \nearrow \zeta^*$, which corresponds to an exponential divergence of the length $a_\perp$ [34]. In the limit $|\zeta - \zeta^*| \gg 1$ the thickness of the adsorption layer is much smaller than R and both the fraction density P and the length $a_\perp$ exhibit in all cases the limiting behavior $P \simeq 2|c|$ and $a_\perp \simeq 1/|c|$ known from a planar surface. This crossover scaling behavior for an ideal chain near the adsorbing generalized cylinder is expected to be universal, i.e., to apply quantitatively also for the asymptotic (large scale) behavior of lattice models [23]. It turns out that the universal asymptotic scaling functions are easily accessible within the present continuum approach.

(6) The behavior of the number of adsorbed monomers at the adsorption threshold $\zeta = \zeta^*$ as a function of $\lambda = L/R^2$ is shown in Fig. 4 for an ideal chain in terms of the scaling function Λ_S defined in Eq. (2.23). The curves display the crossover from the planar limit $L/R^2 \ll 1$ to the long-chain limit $L/R^2 \gg 1$ for which we have obtained analytical results [see Eq. (2.22)].

We conclude by discussing in which cases in the presence of EVI the adsorption-desorption transition, i.e., the formation of a finite adsorbed monomer fraction as $\mathcal{R}$ diverges, survives for an attractive surface with $c < c^*$. As long as $d \leq D-1$ (planar or cylindrical boundary in $D=3$ and straight line boundary in $D=2$) [10], we expect that the transition always occurs because the chain has the possibility to grow *along* the remaining $\delta = D-d \geq 1$ infinitely extended dimensions, thus effectively avoiding contact with itself. For the phase diagram in Fig. 2(a) of the Gaussian field theory this means that the line $p_\alpha(\zeta)$ for $d=2$ is the Gaussian approximation of an experimentally accessible phase transition line, which in the presence of EVI corresponds to the limit $N \to 0$ of the N-component field theory in the outer space of a cylinder in $D=3$ with $\delta = 1$ [56]. In particular the existence of the transition has been proven rigorously [57] for the planar case $D=2$, $d=1$ with $\delta = 1$. However, for $d=D$ excluded volume effects will become so severe [10] that a finite limit of the adsorbed monomer fraction is not possible and a true phase transition will not occur.

Note added in proof. Recently we received a copy of unpublished work by Ch. Hiergeist and R. Lipowsky (HL) [Max-Planck-Institut für Kolloid- und Grenzflächenforschung, Teltow-Seehof, Germany report (1996)] in which polymers are considered that are anchored with one end to a repulsive surface. In a small curvature expansion fro the mushroom regime not only the spontaneous curvature term (see Ref. [40]) but also the rigidity terms $\propto 1/R_m^2$ and $\propto 1/(R_1 R_2)$ have signs that are different from those in the free polymer case considered in the present paper, compare Eq. (32) of HL with our Eq. (C1). For the convenience of the reader we note the form $M_E^{\mathrm{lin}} = (\rho - 1)[(\pi\lambda)^{-1/2} + (d-1)/2 + (\lambda/\pi)^{1/2}(d-1)(d-3)/4 + \cdots]$ of M_E in the linear region [compare Fig. 5(a)] which determines the partition function of an ideal chain that is anchored close to the surface of a weakly curved generalized cylinder. For $d=1$, 2, and 3 this leads to the partition function given in HL for a half sapce (HS), cylinder, and sphere, respectively, and to the corresponding free energy differences $k_B T \ln[M_E^{\mathrm{lin}}/(M_E^{\mathrm{lin}})_{\mathrm{HS}}]$ in which $\rho - 1$ drops out.

APPENDIX A: SURFACE POTENTIAL AND EXTRAPOLATION LENGTH

We are interested either in a purely repulsive surface of the generalized cylinder K in Eq. (1.1) so that Z_L vanishes at the boundary (which may formally be described by the limit $c = +\infty$) or in the neighborhood of the adsorption threshold where the extrapolation length $1/c$ [1,2] is much larger than microscopic lengths such as the range b of the attractive part of the surface potential [18].

In an effort to analyze explicitly the origin of c near the adsorption threshold for the geometry (1.1) we add a short-ranged attractive surface potential $W(r_\perp)$ inside the bracket of the diffusion equation (1.2a):

$$W(r_\perp) = \begin{cases} +\infty, & r_\perp < R-b \\ -w, & R-b < r_\perp < R \\ 0, & R < r_\perp, \end{cases} \quad \text{(A1)}$$

with $w > 0$. This leads to a Laplace transform G of Z_L, which has the form given by Eq. (B3) of Appendix B. However, for $R-b < r_\perp^{(<)} < R$ the quantity

$$(r_\perp^{(<)})^{-\alpha}\left[I_{\alpha+\ell}(\sqrt{\mu}\,r_\perp^{(<)}) - A_\ell^{(\alpha)} K_{\alpha+\ell}(\sqrt{\mu}\,r_\perp^{(<)})\right]$$

on the rhs of Eq. (B.3c) has to be replaced by a dependence on $r_\perp^{(<)}$ proportional to

$$Q(r_\perp^{(<)}) = \frac{1}{2i}(r_\perp^{(<)})^{-\alpha}\left\{ \frac{H_{\alpha+\ell}^{(1)}(\sqrt{\mu_b}\,r_\perp^{(<)})}{H_{\alpha+\ell}^{(1)}[\sqrt{\mu_b}(R-b)]} \right. $$
$$\left. - \frac{H_{\alpha+\ell}^{(2)}(\sqrt{\mu_b}\,r_\perp^{(<)})}{H_{\alpha+\ell}^{(2)}[\sqrt{\mu_b}(R-b)]} \right\}, \quad \text{(A2)}$$

where $\mu_b \equiv w - p^2 - t$ and $H_\alpha^{(1)}$, $H_\alpha^{(2)}$ denote Hankel functions [25]. The logarithmic derivative of Q with respect to $r_\perp^{(<)}$ at $r_\perp^{(<)} = R$ defines c. Since near the threshold one has for R/b large [18]

$$\sqrt{\mu_b}\,R \simeq \pi R/(2b) \quad \text{(A3)}$$

the Hankel functions attain their asymptotic form for which the dependence on $\alpha + \ell$ drops out. There remains, however, a dependence on d from the prefactor $(r_\perp^{(<)})^{-\alpha}$ on the rhs of Eq. (A2) so that

$$c \simeq \frac{\pi}{2}\left(\frac{\pi}{2b} - \sqrt{w}\right) - \frac{d-1}{2R} \quad \text{(A4)}$$

apart from a negligible contribution $\propto b(p^2 + t)$.

Using the threshold values c^*, which follow from Eq. (2.9a) one finds

$$\frac{\pi}{2}\left(\frac{\pi}{2b}-\sqrt{w^*}\right)\simeq\begin{cases}(d-1)/(2R), & d\leq 2 \\ (3-d)/(2R), & d>2,\end{cases} \quad (A5)$$

so that the threshold value w^* of w in $W(r_\perp)$ depends on d. In particular $w^*=w^*(d)$ is smallest for $d=2$ and $w^*(3)=w^*(1)$, which is consistent with the results of Ball, Blunt, and Barford [58].

Equation (A4) shows that the description of the surface of K (which has a constant curvature) by means of a logarithmic derivative or inverse extrapolation length c also encompasses the asymptotic behavior near the adsorption threshold of the particular model (A1). The quantity c enters into measurable quantities in a much more direct and universal way than potential distributions in a continuum model (or energy gains in surface layers of a lattice model). In this work we assume that c has a given value and thus we avoid the complicated task of calculating c for a particular curved surface exposed to a specific polymer system.

APPENDIX B: THE GAUSSIAN PROPAGATOR

The Gaussian two-point correlation function in the volume V as introduced in Eq. (1.1) satisfies the Schrödinger-type equation [22]

$$(-\Delta_D+t)G(\mathbf{r},\mathbf{r}';t,c,R)=\delta^{(D)}(\mathbf{r}-\mathbf{r}') \quad (B1a)$$

with the boundary condition

$$\partial_n G(\mathbf{r},\mathbf{r}';t,c,R)|_{\mathbf{r}=\mathbf{r}_S}=cG(\mathbf{r},\mathbf{r}';t,c,R)|_{\mathbf{r}=\mathbf{r}_S}, \quad (B1b)$$

where $\mathbf{r}_S$ is a point on the surface of K. In order to solve Eq. (B1) we first note that the Laplacian operator Δ_D in coordinates adapted to our specific problem has the form (D and d are integers)

$$\Delta_D=\Delta_d+\sum_{i=1}^{\delta}\frac{\partial^2}{\partial r_{\parallel,i}^2}, \quad (B2a)$$

where $\delta=D-d$ and

$$\Delta_d=\frac{\partial^2}{\partial r_\perp^2}+\frac{d-1}{r_\perp}\frac{\partial}{\partial r_\perp}+\frac{1}{r_\perp^2}\left[\frac{\partial^2}{\partial\vartheta^2}+(d-2)\cot\vartheta\frac{\partial}{\partial\vartheta}\right] \quad (B2b)$$

is the Laplacian operator in the d-dimensional subspace $\{\mathbf{r}_\perp\in\mathbb{R}^d;r_\perp>R\}$ in spherical coordinates. Here ϑ denotes the angle of the coordinate $\mathbf{r}_\perp$ with respect to a fixed direction in the radial subspace (see Fig. 1). (For $d=1$ there is no angle ϑ so that in this case the term in square brackets must be omitted.)

Using a well-known technique [59] for solving Eq. (B1) we eventually arrive at

$$G(\mathbf{r},\mathbf{r}';t,c,R)\equiv G(r_\perp,r_\perp',\vartheta,|\mathbf{r}_\parallel-\mathbf{r}_\parallel'|;t,c,R)=\sum_{\ell=0}^{\infty}W_\ell^{(\alpha)}(\vartheta)\int_{\mathbb{R}^\delta}\frac{d^\delta p}{(2\pi)^\delta}\exp[i\mathbf{p}(\mathbf{r}_\parallel-\mathbf{r}_\parallel')]\widetilde{G}_\ell(r_\perp,r_\perp';\mu,c,R), \quad d<D,$$

$$=\sum_{\ell=0}^{\infty}W_\ell^{(\alpha)}(\vartheta)\widetilde{G}_\ell(r_\perp,r_\perp';t,c,R), \quad d=D, \quad (B3a)$$

where $\alpha\equiv(d-2)/2$ and $\mu\equiv p^2+t$. The last line holds because for $d=D$ there is no parallel component $\mathbf{r}_\parallel-\mathbf{r}_\parallel'$ and hence no Fourier variable $\mathbf{p}$. The function $W_\ell^{(\alpha)}(\vartheta)$ is given by

$$W_\ell^{(\alpha)}(\vartheta)=\begin{cases}(2\pi^{d/2})^{-1}\Gamma(\alpha)(\ell+\alpha)C_\ell^\alpha(\cos\vartheta), & d\neq 2, \\ (2\pi)^{-1}(2-\delta_{\ell,0})\cos(\ell\vartheta), & d=2,\end{cases} \quad (B3b)$$

where Γ is the Γ function, C_ℓ^α denote Gegenbauer polynomials [25], and $\delta_{\ell,0}=1$ for $\ell=0$ and zero otherwise. Here $W_\ell^{(\alpha)}(\vartheta)$ is normalized so that $\int d\Omega_d W_\ell^{(\alpha)}=\delta_{\ell,0}$. The second line of Eq. (B3b) is the limit $d\to 2$ of the first line. The propagator $\widetilde{G}_\ell$ takes the form

$$\widetilde{G}_\ell(r_\perp,r_\perp';\mu,c,R)=(r_\perp^{(<)}r_\perp^{(>)})^{-\alpha}K_{\alpha+\ell}(\sqrt{\mu}r_\perp^{(>)})[I_{\alpha+\ell}(\sqrt{\mu}r_\perp^{(<)})-A_\ell^{(\alpha)}(\mu,c,R)K_{\alpha+\ell}(\sqrt{\mu}r_\perp^{(<)})], \quad (B3c)$$

where $r_\perp^{(<)}\equiv\min(r_\perp,r_\perp')$ and $r_\perp^{(>)}\equiv\max(r_\perp,r_\perp')$. For $d=D$ the variable μ is to be replaced by t. I_α and K_α denote modified Bessel functions [25] and

$$A_\ell^{(\alpha)}(\mu,c,R)=\frac{\sqrt{\mu}RI_{\alpha+\ell+1}(\sqrt{\mu}R)+(\ell-cR)I_{\alpha+\ell}(\sqrt{\mu}R)}{-\sqrt{\mu}RK_{\alpha+\ell+1}(\sqrt{\mu}R)+(\ell-cR)K_{\alpha+\ell}(\sqrt{\mu}R)} \quad (B3d)$$

(see also Refs. [60], [24], and [28]).

We note that in the case $d=1$ only the terms with $\ell=0$ and 1 appear on the rhs of Eq. (B3a) and yield the well-known Gaussian propagator for the semi-infinite space $r_\perp>R$ [4,22,61]

$$G(r_\perp,r_\perp',|\mathbf{r}_\parallel-\mathbf{r}_\parallel'|;t,c)=\int_{\mathbb{R}^{D-1}}\frac{d^{D-1}p}{(2\pi)^{D-1}}\exp[i\mathbf{p}(\mathbf{r}_\parallel-\mathbf{r}_\parallel')]\frac{1}{2\sqrt{\mu}}\left[e^{-\sqrt{\mu}|r_\perp-r_\perp'|}-\frac{c-\sqrt{\mu}}{c+\sqrt{\mu}}e^{-\sqrt{\mu}(r_\perp+r_\perp'-2R)}\right]. \quad (B4)$$

Finally we note that the usual Gaussian propagator G_b in the D-dimensional unbounded bulk space is given by Eq. (B3) with $A_{\ell}^{(\alpha)}(\mu,c,R)=0$. In this case the summation over ℓ and the integration over $\mathbf{p}$ can be carried out explicitly yielding the well-known result

$$G_b(|\mathbf{r}-\mathbf{r}'|;t)=(2\pi)^{-D/2}t^{(D-2)/4}\frac{K_{(D-2)/2}(\sqrt{t}|\mathbf{r}-\mathbf{r}'|)}{|\mathbf{r}-\mathbf{r}'|^{(D-2)/2}}. \tag{B5}$$

APPENDIX C: SMALL-CURVATURE EXPANSION FOR A REPULSIVE SURFACE OF GENERAL SHAPE

A small-curvature expansion such as (3.9) is also expected for a particle $\mathcal{K}$ of *more general shape* provided its surface S is smooth and all principal radii of curvature are much larger than the chain end-to-end distance $\mathcal{R}$ [20] (compare the related discussions in Refs. [62] and [12](c)]).

We consider a particle $\mathcal{K}$ in $D=3$ with finite volume $v_{\mathcal{K}}$ and with a purely repulsive boundary surface $S=\partial\mathcal{K}$ immersed in a dilute solution of ideal chains. Due to general arguments [63] the expression $F_{\mathcal{K}}/p_0-v_{\mathcal{K}}$ corresponding to Eqs. (3.6c) and (3.9) is expected to take the usual form of a surface integral over the local surface free energy density and the first- and second-order local curvature energy densities, i.e.,

$$F_{\mathcal{K}}/p_0-v_{\mathcal{K}}=\int_S dS\left\{\frac{2}{\sqrt{\pi}}L^{1/2}+\frac{L}{R_m}-\frac{2L^{3/2}}{3\sqrt{\pi}}\left[\frac{1}{R_m^2}-\frac{1}{R_1R_2}\right]\right.$$
$$\left.+\cdots\right\}, \tag{C1}$$

where R_1, R_2 are the two principal local radii of curvature,

$$\frac{1}{R_m}=\frac{1}{2}\left(\frac{1}{R_1}+\frac{1}{R_2}\right) \tag{C2}$$

is the mean local curvature, and $1/(R_1R_2)$ is the local Gaussian curvature. (We use the convention that $R_1,R_2>0$ means that the boundary surface is bent *away* from the polymer solution located in the exterior of $\mathcal{K}$.) We note that

$$\frac{1}{R_m^2}-\frac{1}{R_1R_2}=\frac{1}{4}\left(\frac{1}{R_1}-\frac{1}{R_2}\right)^2\geq 0. \tag{C3}$$

The prefactors (curvature energies) of the terms $1/R_m$, $1/R_m^2$ and $1/(R_1R_2)$ on the rhs of Eq. (C1) are uniquely determined by the special cases that $\mathcal{K}$ is a sphere ($R_1=R_2=R$) and that $\mathcal{K}$ is a cylinder ($R_1=R$, $R_2=\infty$) and follow by the comparison with Eq. (3.9) for $d=3$ and $d=2$, respectively.

The rhs of Eq. (C1) determines also the change in surface free energy and in the first- and second-order curvature energies of a *flexible* surface such as a *membrane* upon exposing one side of it to a solution of ideal polymers [62(d),(e)], which are repelled by the surface. Thus the addition of polymers favors a bending of the membrane surface *towards* the solution [40] and leads to a *weakening* of its surface rigidity. The sign of the Gaussian curvature energy will generally favor surfaces with higher genuses and thus the formation of handles.

These predictions are opposite to some of the conclusions in Refs. [62(d),(e)] [see in particular Eq. (12) and the text below Eq. (13) in Ref. [62(d)]]. For an examination and explanation of this discrepancy see Ref. [64].

[1] P. G. de Gennes, *Scaling Concepts in Polymer Physics* (Cornell University, Ithaca, 1979).

[2] P. G. de Gennes, Rep. Prog. Phys. **32**, 187 (1969).

[3] *Physics of Polymer Surfaces and Interfaces*, edited by I. C. Sanchez (Butterworth-Heinemann, Boston, 1992).

[4] E. Eisenriegler, *Polymers near Surfaces* (World Scientific, Singapore, 1993).

[5] K. De'Bell and T. Lookman, Rev. Mod. Phys. **65**, 87 (1993).

[6] G. Fleer, M. Cohen-Stuart, J. Scheutjens, T. Cosgrove, and B. Vincent, *Polymers at Interfaces* (Chapman and Hall, London, 1993).

[7] D. H. Napper, *Polymeric Stabilization of Colloidal Dispersions* (Academic, London, 1989).

[8] J. Buitenhuis, L. N. Donselaar, P. A. Buining, A. Stroobants, and H. N. Lekkerkerker, J. Colloid Interface Sci. **175**, 46 (1995).

[9] R. Lipowsky, Europhys. Lett. **30**, 197 (1995).

[10] P. A. Pincus, C. J. Sandroff, and T. A. Witten, Jr., J. Phys. (Paris) **45**, 725 (1984).

[11] (a) S. Boettcher and M. Moshe, Phys. Rev. Lett. **74**, 2410 (1995); (b) S. Boettcher, Phys. Rev. E **51**, 3862 (1995); (c) C. M. Bender, F. Cooper, and P. N. Meisinger (unpublished); (d) C. M. Bender, S. Boettcher, and P. N. Meisinger (unpublished).

[12] (a) S. Alexander, J. Phys. (Paris) **38**, 977 (1977); (b) C. M. Marques and J. F. Joanny, *ibid.* **49**, 1103 (1988); (c) J. T. Brooks, C. M. Marques, and M. E. Cates, J. Phys. (France) II **1**, 673 (1991); (d) C. M. Wijmans, F. A. M. Leermakers, and G. J. Fleer, Langmuir **10**, 1331 (1994); (e) L. Picullel, C. Viebke, and P. Linse, J. Phys. Chem. **99**, 17423 (1995).

[13] (a) R. Toral and A. Chakrabarti, Phys. Rev. E **47**, 4240 (1993); (b) C. M. Wijmans and E. B. Zhulina, Macromolecules **26**, 7214 (1993); (c) J. M. R. d'Oliveira, J. M. G. Martinho, R. Xu, and M. A. Winnik, *ibid.* **28**, 4750 (1995).

[14] E. J. Meijer and D. Frenkel, J. Chem. Phys. **100**, 6873 (1994); Phys. Rev. Lett. **67**, 1110 (1991).

[15] C. M. Wijmans, F. A. M. Leermakers, and G. J. Fleer, Langmuir **10**, 4514 (1994); D. R. M. Williams and F. C. MacKin-

tosh, J. Phys. (France) II **5**, 1407 (1995).

[16] J. des Cloizeaux and G. Jannink, *Polymers in Solution* (Clarendon, Oxford, 1990).

[17] (a) T. W. Burkhardt and E. Eisenriegler, Phys. Rev. Lett. **74**, 3189 (1995); (b) E. Eisenriegler and U. Ritschel, Phys. Rev. B **51**, 13717 (1995).

[18] The behavior of a long flexible chain on large spatial scales is to a great extent independent of microscopic details. The continuum description is designed to capture these large scale universal properties. In our particular situation dependences on the polymer end-to-end distance $\mathcal{R}$ [20], the radius R of the generalized cylinder, and distances $r_\perp - R$ from the surface will only be universal if these lengths are much larger than microscopic lengths such as the lattice constant in a lattice based walk model (or the bead size in a freely jointed bead model) and the range of the attractive surface potential.

[19] Generally $Z_L(\mathbf{r}, \mathbf{r}')$ denotes the *ratio* of the partition function of a chain with two fixed ends in the presence of the boundary (and, possibly, of EVI) and the partition function of an ideal chain in the unbounded bulk space with one end position integrated. Thus it has the dimension of an inverse volume. For an ideal chain in the unbounded D-dimensional space Z_L is a Gaussian distribution $Z_{L,b}^{(D)}(|\mathbf{r} - \mathbf{r}'|) = (4\pi L)^{-D/2} \exp[-|\mathbf{r} - \mathbf{r}'|^2/(4L)]$, which is normalized so that $\int_{\mathbb{R}^D} d^D r Z_{L,b}^{(D)} = \hat{Z}_{L,b}^{(D)} = 1$. The same Gaussian distribution appears in the form $Z_{L,b}^{(\delta)}(|\mathbf{r}_\parallel - \mathbf{r}'_\parallel|)$ in Eq. (1.3) and characterizes the dependence on the parallel spatial components. For the perpendicular components, however, it appears only in the limit $r_\perp - R \to \infty$ with $|\mathbf{r}_\perp - \mathbf{r}'_\perp|$, L, and c kept fixed for which $Z_L^{(\perp)}(\mathbf{r}_\perp, \mathbf{r}'_\perp; c, R) \to Z_{L,b}^{(d)}(|\mathbf{r}_\perp - \mathbf{r}'_\perp|)$.

[20] The precise meaning of L is given by the relation $\mathcal{R}^2 = 2LD$ involving the root-mean-square end-to-end distance $\mathcal{R}$ of the ideal chain in unbounded D-dimensional space as follows from Eq. (1.2) (compare, e.g., Ref. [16]).

[21] K. Binder, in *Phase Transitions and Critical Phenomena*, edited by C. Domb and J. L. Lebowitz (Academic, London, 1983), Vol. 8, p. 1.

[22] H. W. Diehl, in *Phase Transitions and Critical Phenomena*, edited by C. Domb and J. L. Lebowitz (Academic, London, 1986), Vol. 10, p. 75.

[23] The relationship between the layer density $m_\diagup$ of the monomer fraction ''near'' the surface and c, R, and $\mathcal{R}$ [20] is expected to be *universal*, i.e., the result for $m_\diagup$ that follows from Eq. (1.7) applies quantitatively also for a lattice (or freely jointed bead) model for an ideal chain provided the small lengths $y_\perp - R$ and $dy_\perp$ are still large compared to microscopic lengths [18]. The situation is different in the case of the dependence $n_S \propto L m_\diagup$ of the number n_S of surface contacts (monomers that are microscopically close to the surface) on c, R, and the total monomer number $n \propto L$ because this dependence is universal only apart from nonuniversal scale factors. The layer density $m_\diagup$ has the dimension of an inverse length; for a planar surface the quantities $L m_\diagup$ and $L m(\mathbf{y})$ correspond to the quantities $\langle m^\lambda(0) \rangle$ and $\langle m(\mathbf{y}) \rangle$ introduced in *Polymers near Surfaces* (Ref. [4]), Chap. III.

[24] For Dirichlet boundary conditions $c = +\infty$ the Gaussian propagator for the interior and exterior of a spherical ($d = D$) surface in D dimensions has been obtained in E. Eisenriegler, Z. Phys. B **61**, 299 (1985).

[25] M. Abramowitz and I. A. Stegun, *Handbook of Mathematical Functions* (Dover, New York, 1972); I. S. Gradshteyn and I.

M. Ryzhik, *Table of Integrals, Series, and Products* (Academic, London, 1965).

[26] Note that for $\alpha = -1/2$ and $\alpha = 1/2$ (i.e., $d = 1$ and $d = 3$) the Bessel functions reduce to elementary functions so that most of the calculations can be carried out explicitly.

[27] Compare with P. J. Upton, J. O. Indekeu, and J. M. Yeomans, Phys. Rev. B **40**, 666 (1989). These authors consider a Ginzburg-Landau model that follows from the Hamiltonian (1.5) by adding a Φ^4 interaction in the bulk and symmetry breaking bulk and surface interactions linear in Φ in order to study wetting phenomena on spherical and cylindrical substrates. Their line of surface transitions [21,22], which they find within the mean-field approximation coincides with our boundary lines $\tau = p_\alpha(\zeta)$, $\zeta < \zeta^*$ in the phase diagram of the Gaussian model; compare their Eqs. (5.7) and (5.10) with our Eqs. (2.8), (2.9) for $d = 3$ and $d = 2$, respectively.

[28] For a sphere in $D = d > 2$ at the bulk critical temperature $T = T_c^b$ one finds that the Gaussian two-point correlation function G is *conformal invariant* for (and only for) the boundary conditions $\zeta \equiv \zeta_O = +\infty$ and $\zeta \equiv \zeta_{SB} = -(d-2)/2$ [see, e.g., Ref. [17(b)]]. This can be checked explicitly if one notes that for $t = 0$ and $d > 2$ Eq. (B3c) reads $\widetilde{G}_\diagup = (r_\perp^{(<)} r_\perp^{(>)})^{-\alpha} (r_\perp^{(>)}/R)^{-(\alpha + \diagup)} [(r_\perp^{(<)}/R)^{\alpha + \diagup} + D_\diagup^{(\alpha)}(\zeta)(r_\perp^{(<)}/R)^{-(\alpha + \diagup)}]/[2(\alpha + \diagup)]$ with $D_\diagup^{(\alpha)}(\zeta) = (\diagup - \zeta)/(\diagup + 2\alpha + \zeta) = \pm 1$ for $\zeta = \zeta_O$ (lower sign) and $\zeta = \zeta_{SB}$ (upper sign), respectively. This leads to the form $G = [\Gamma(\alpha)/(4\pi^{d/2})]|\mathbf{r} - \mathbf{r}'|^{-2\alpha}[1 \pm (1 + y)^{-\alpha}]$ with the conformal invariant combination $y = (r^2 - R^2)(r'^2 - R^2)/(R^2 |\mathbf{r} - \mathbf{r}'|^2)$, which has been obtained in T. W. Burkhardt and E. Eisenriegler, J. Phys. A **18**, L83 (1985). Note that the value ζ^* found in Eq. (2.9a) where $D_{\diagup = 0}^{(\alpha)}$ and G diverge is *different* from ζ_{SB}, in accordance with the fact that G is finite for $D = d > 2$ and $(t = 0, \zeta = \zeta_{SB})$.

[29] For a table of inverse Laplace transforms see, e.g., *Tables of Integral Transforms*, edited by A. Erdélyi (McGraw-Hill, New York, 1954), Vol. I.

[30] Equation (2.15) reproduces the known result for the planar case $d = 1$ [see, e.g., Eq. (3.77) in Ref. [4]] and for $d = 3$ it contains as a special case the result presented in Eq. (6) in Ref. [9] for a purely repulsive surface $\zeta = +\infty$.

[31] Since $p_\alpha(\zeta)$ does not depend on ρ the adsorbed fraction density $P(c, R)$ does *not* depend on the radial component $r_\perp$ of the point where one end of the chain is fixed. Intuitively this is clear because the Gaussian chain must eventually reach the surface as the chain length L increases. However, the *approach* to that limit strongly depends on $r_\perp$ in that the chain for $c < c^*$ suddenly ''jumps'' onto the surface [see Eq. (3.82) and the discussion between Eqs. (3.84) and (3.85) in Ref. [4] for the planar case $d = 1$].

[32] It would be interesting to investigate the adsorption of a single chain onto a cylindrical surface ($d = 2$) if EVI is present (compare the discussion at the end of Sec. V). While we believe that an adsorption transition still exists in this case we do not expect that the transition occurs in the exceptional form of an essential singularity [Eq. (2.19)].

[33] By inserting in Ref. [11(b)] Eqs. (50), (33) and (41), (42) into Eq. (40) we realized that for $m \gg 1$ (but $m\Delta\kappa \ll 1$) the quantity Δz on the lhs of Eq. (44) should actually be replaced by the product $m^2 \Delta z$. This product arises from the argument in the first term, $-\ln[4\sqrt{3} m (\Delta z)^{1/2}]$, on the rhs of Eq. (50). Apart from dimensionless nonuniversal prefactors of order unity the

quantities $m^2 \Delta z$ and $m \Delta \kappa$ in Refs. [11(a),(b)] correspond to our scaled variables p_α and $\Delta \zeta$, respectively.

[34] The exponential growth of the mean distance $a_\perp$ of a flexible line that unbinds from a cylinder has been observed before by Pincus, Sandroff, and Witten [10] and, within a slightly different context, by M. Vallade and J. Lajzerowicz, J. Phys. (Paris) **42**, 1505 (1981) and by R. Lipowsky, Europhys. Lett. **15**, 703 (1991).

[35] For a dilute solution of chains with EVI the bulk-normalized end density is also given by the ratio of single chain partition functions with one end free in the presence and absence of the generalized cylinder K, respectively, and displays a similar scaling form $M_E = M_E(\rho; \mathcal{R}/R)$. Here $\mathcal{R}$ is the root-mean-square end-to-end distance of a chain with EVI in unbounded bulk, which is proportional to L^ν [1,16] with $\nu \approx 0.59$ in $D = 3$. The functions $\hat{\mathcal{Z}}_\lambda$, $\hat{\mathcal{Z}}_{\lambda,b}^{(D)}$ and M_E for chains with EVI differ from those for ideal chains [see, e.g., Eq. (4.12)].

[36] A similar behavior is also expected for a dilute solution of chains with EVI if $\mathcal{R}/R$ is small. In particular, for $r_\perp - R \ll \mathcal{R} \ll R$, we expect $M_E \propto (r_\perp - R)^{a'}$ where $a' \approx 0.82$ in $D = 3$ (instead of $a' = 1$ for ideal chains). The exponent a' is given by the difference of the bulk and surface exponent of the order parameter Φ of the field theory in a half space [4]. [The estimate $a' = (1/2)(\eta_{\parallel,\text{ord}} - \eta) \approx 0.82$ has been obtained using the value ≈ 1.66 for the critical surface exponent $\eta_{\parallel,\text{ord}}$ given in H. W. Diehl and M. Shpot, Phys. Rev. Lett. **73**, 3431 (1994).] For the monomer density M_M the corresponding exponent is the inverse $1/\nu \approx 1.70$ of the bulk exponent ν [1,4].

[37] It is interesting to analyze the corresponding behavior near a cylinder in $D = 3$ if the chain is endowed with EVI. In Sec. IV we shall argue that the limit of M_E for $\mathcal{R} \to \infty$ is also *finite* for ($D = 3$, $d = 2$) and shall discuss its behavior for $\rho \gg 1$.

[38] Here we refer to generalized cylinders K with a nonvanishing number $\delta = D - d > 0$ of (parallel) directions where the extent is infinite such as a (uniaxial) cylinder with $\delta = 1$ or a plate bounded by two parallel planar surfaces with $\delta = D - 1$. In these cases one may choose $\mathcal{V}_\parallel = \lambda_\parallel^\delta$ where $\lambda_\parallel$ is the length of the cylinder axis or the lateral extension of the plate. For $\mathcal{K} = K$ a *sphere* ($\delta = 0$) there is no parallel subspace and the evaluation of the free energy $F_\mathcal{K}$ is even simpler; the result is $F_\mathcal{K} = p_0 \delta f_K$ with δf_K from Eq. (3.7) and follows formally from Eq. (3.6) by putting $\mathcal{V}_\parallel = 1$.

[39] For the plate geometry ($d = 1$) [38] the factor $\Omega_{d=1} = 2$ in front of the curly bracket in Eq. (3.9) accounts for the *two* planar surfaces.

[40] This is plausible because a surface that is bent away from the polymer solution leads to an *increase* of the depletion layer effect (compare the discussion for the corresponding magnetic system near Eq. (2.24) in the reference cited in Ref. [24]). The present situation of *free* polymers should be distinguished from the case in which a (single) polymer is *anchored* with one end to the repulsive surface. The latter case favors a bending of the surface *away* from the polymer [9].

[41] S. Asakura and F. Oosawa, J. Polym. Sci. **33**, 183 (1958); for a recent application of the phs approximation see P. B. Warren, S. M. Ilett, and W. C. K. Poon, Phys. Rev. E **52**, 5205 (1995).

[42] As will be shown in Eq. (4.14), for systems with a positive exponent $d - \nu^{-1}$ (such as a cylinder in $D = 3$ in case of EVI or a sphere) one has generally $\delta f_K \sim \mathcal{R}^{1/\nu} R^{d-(1/\nu)}$ for $R \to 0$. The phs result $\delta f_K^{(\text{phs})} \sim \mathcal{R}^d$ for $R \to 0$ does not depend on R in

this limit and thus $\delta f_K^{(\text{phs})}$ is too large by a factor $(\mathcal{R}/R)^{d-(1/\nu)}$.

[43] This effect has also been observed within the approximate treatment of Ref. [12(e)].

[44] The ''small'' radius must, however, be large on a microscopic scale [18].

[45] For an appropriate generalization of the Gaussian model [Eq. (1.5)] for chains with EVI see Refs. [1,4,16] and Sec. V.

[46] In a field-theoretic description [16,4] this arises from the fact that both Φ^2 and L need the *same* renormalization factor, which drops out in the ratio Φ^2/L.

[47] (a) D. J. Amit, *Field Theory, the Renormalization Group, and Critical Phenomena* (McGraw-Hill, New York, 1978); (b) J. Zinn-Justin, *Quantum Field Theory and Critical Phenomena* (Clarendon, Oxford, 1989); (c) J. L. Cardy, in *Phase Transitions and Critical Phenomena*, edited by C. Domb and J. L. Lebowitz (Academic, London, 1986), Vol. 11, p. 55.

[48] For $r_\perp \ll \mathcal{R}$ the integral containing $\Phi^2(\mathbf{y})$ on the rhs of Eq. (4.3c) is dominated by the region where Eq. (4.11) holds.

[49] Equation (4.1) is a local property and applies, with the same amplitude $\mathcal{A}_K$ and exponent x_K, within bulk or half-space averages. In the latter case the argument of Φ^2 must be an interior point of the half space.

[50] P. R. Sperry, H. B. Hopfenberg, and N. L. Thomas, J. Colloid Interface Sci. **82**, 62 (1980).

[51] H. N. W. Lekkerkerker, J. K. G. Dhont, H. Verduin, C. Smits, and J. S. van Duijneveldt, Physica A **213**, 18 (1995); (b) W. C. K. Poon and P. N. Pusey, in *Observation, Prediction, and Simulation of Phase Transitions in Complex Fluids*, Vol. 460 of *NATO Advanced Study Institute, Series C: Mathematical and Physical Sciences*, edited by M. Baus, L. R. Rull, and J. P. Ryckaert (Kluwer Academic, Dordrecht, 1995), p. 3; (c) H. N. W. Lekkerkerker, P. Buining, J. Buitenhuis, G. J. Vroege, and A. Stroobants, *ibid.*, p. 53.

[52] Actually we have considered a more general ''particle,'' namely, a generalized cylinder K [see Eq. (1.1)], which comprises planar, cylindrical, or spherical boundaries as special cases.

[53] The ground-state-dominance approximation [1] is sufficient for studying the behavior for $L \to \infty$ at $c < c^*$, e.g., the thickness $a_\perp$ of the adsorption layer [10], or the adsorption fraction density $\mathcal{P}(\zeta)$ in the adsorbed limit [11]. On the other hand, it is not valid for other important quantities such as $\hat{\lambda}_S(\rho; \lambda, \zeta)$ at $\zeta = \zeta^*$ and its crossover behavior with increasing $\lambda = L/R^2$, or for the density profiles M_E and M_M for a purely repulsive surface $c = +\infty$. In Ref. [9] the full partition function $\hat{Z}_L$ is considered for the special case of a purely repulsive sphere.

[54] In general, SDEs can be written in ''operator form.'' In the planar case $d = 1$ Eq. (5.1) corresponds to the operator expansion [22] $\Phi(z, \mathbf{s}) = \Sigma_k A_k z^{a_k} \sigma_k(\mathbf{s})$ with $z = r_\perp - R$ and for which the lowest surface operator $\sigma_1(\mathbf{s}) = \partial_z \Phi(z, \mathbf{s})_{z=0}$ has a scaling dimension that within the Gaussian model is by the amount $a_1 = 1$ larger than that of Φ. The quantities A_k are amplitudes. A term $\propto z^2$ cannot occur because the corresponding possible surface operators $\sigma_{2,A} = (\partial_z^2 \Phi)_{z=0}$ and $\sigma_{2,B} = (\Delta_\mathbf{s} \Phi)_{z=0}$ vanish for a planar surface with Dirichlet conditions. This is obvious for $\sigma_{2,B}$ and follows for $\sigma_{2,A}$ from the ''equation of motion'' $\sigma_{2,A} = -\sigma_{2,B} + t\Phi|_{z=0} = -\sigma_{2,B}$. In the case of a curved surface with finite radius R and with $\mathbf{s}$ tangential to the surface this relation still applies but $\sigma_{2,B}$ does not vanish and can be expressed in terms of σ_1/R [see Eq. (B2)], which implies an

operator form that corresponds to Eq. (5.1). We expect that these arguments can be appropriately generalized to a theory including a $|\Phi|^4$ interaction.

[55] In the operator expansion [54] this term could be included as an additional operator-free contact term that contributes only to integrals over correlation functions of low order.

[56] While systems with $N<1$ can order spontaneously in one infinitely extended dimension [see, e.g., R. Balian and G. Toulouse, Ann. Phys. (N.Y.) **83**, 28 (1974)], in contrast Ising-like ($N=1$) systems (or models with $N\geq 2$) reveal a spontaneous magnetization only if more than one (than two) infinitely extended dimensions are present. Thus in the physical ($D=3$)-dimensional space the surface of the generalized cylinder K with $\delta=3-d$ infinitely extended dimensions cannot order by itself—and there will be no surface transition [21,22] — if $N\geq 1$ and $d\geq 2$. [For an Ising-like system with only one infinitely extended dimension a spontaneous magnetization at finite temperature is prevented by the formation of domains of opposite magnetization; see, e.g., L. D. Landau and E. M. Lifshitz, *Statistical Physics* (Pergamon, London, 1958).] From the finite-size scaling theory of second-order phase transitions we expect that for $D=3$, $d\geq 2$, and $N\geq 1$, e.g., the local susceptibility $\mathcal{X}(\rho;\tau,\zeta)$ displays a *rounded maximum* along lines to which the lines $p_\alpha(\zeta)$ in Fig. 2 (a) are the corresponding Gaussian approximation; this maximum remains finite in the region $\tau>0$ (compare the reference cited in Ref. [27]).

[57] J. M. Hammersley, G. M. Torrie, and S. G. Whittington, J. Phys. A **15**, 539 (1982).

[58] R. C. Ball, M. Blunt, and W. Barford, J. Phys. A **22**, 2587 (1989).

[59] See, e.g., T. C. Lubensky and M. H. Rubin, Phys. Rev. B **12**, 3885 (1975).

[60] In order to obtain the Gaussian propagator for the *interior* of

K one merely has to interchange the symbols K, I, and $r_\perp^{(>)}$, $r_\perp^{(<)}$ on the rhs of Eq. (B.3c) and to replace $A_\ell^{(\alpha)}$ by $B_\ell^{(\alpha)} = [\sqrt{\mu}R K_{\alpha+\ell+1}(\sqrt{\mu}R) - (\ell+cR)K_{\alpha+\ell}(\sqrt{\mu}R)] / [-\sqrt{\mu}R I_{\alpha+\ell+1}(\sqrt{\mu}R) - (\ell+cR)I_{\alpha+\ell}(\sqrt{\mu}R)]$ (compare Ref. [24]).

[61] Analogous to Ref. [60] one can derive the Gaussian propagator for the *film geometry*. This result is given in Eq. (4.1) in Ref. [22].

[62] (a) P. G. de Gennes, J. Phys. Chem. **94**, 8407 (1990); (b) R. Balian and C. Bloch, Ann. Phys. (N.Y.) **60**, 401 (1970); **64**, 271 (1971); **84**, 559 (1974); (c) B. Duplantier, Physica A **168**, 179 (1990); (d) R. Podgornik, Europhys. Lett. **21**, 245 (1993); (e) R. Podgornik, Phys. Rev. E **51**, 3368 (1995).

[63] See, e.g., F. David, in *Statistical Mechanics of Membranes and Surfaces*, edited by D. Nelson, T. Piran, and S. Weinberg (World Scientific, Singapore, 1988).

[64] We examine the reason for the disagreement using notations from Ref. [62(d)]. First, we note that the expression for $\Xi(s)$ on the rhs of Eq. (11) in Ref. [62(d)] with the definition of U in Eq. (10) (with $\kappa=+\infty$) and the definition of $\Xi_0(s)$ below Eq. (6) is *completely consistent* with our Eq. (C1) in Appendix C. However, one has to take into account that the spatial integrations $\int\int d^3\mathbf{R}d^3\mathbf{R}'$ in Ref. [62(d)] have to be performed only over the half-space V_+ occupied by the polymer solution while the other side V_- of the boundary surface has to be excluded from the integration. It seems that in the step that leads from Eq. (11) to Eq. (12) the quantity $B(s) \equiv (1/s)V_+ - \Xi_0(s) = \int_{V_+}\int_{V_-}d^3\mathbf{R}d^3\mathbf{R}' G_0(\mathbf{R},\mathbf{R}';s)$, which contributes to the zeroth- and second-order curvature term, has been neglected. We also note that for the quantity R_ω in Refs. [62(d),(e)] and our quantity R_m in Eq. (C2) an opposite sign convention has been used so that $R_\omega = -R_m$ [compare Fig. 1 and Eq. (21) in Ref. [62(e)]].